

学位論文  
**Doctoral Thesis**

**Mapping neuronal activity in the mouse brain by  
analyzing immediate early gene expression**

(最初期遺伝子の発現解析を用いたマウス脳における  
神経活動マッピング)

アシム クマール ベパリ  
**Asim Kumar Bepari**

熊本大学大学院医学教育部博士課程医学専攻  
発生・再生医学研究者育成コース

指導教員

玉巻 伸章 教授  
熊本大学大学院医学教育部博士課程医学専攻脳回路構造学

## Table of Contents

Summary .....	2
List of reference articles.....	3
Acknowledgments.....	4
List of abbreviations.....	5
Background .....	6
Part-I: Visualization of odor-induced neuronal activity by immediate early gene expression	8
Introduction-I.....	9
Method-I .....	12
Results-I.....	16
Discussion-I .....	38
Part-II: Identification of optogenetically activated striatal medium spiny neurons by <i>Npas4</i> expression .....	45
Introduction-II.....	46
Method-II .....	48
Results-II.....	53
Discussion-II .....	70
Conclusion.....	73
References .....	74

## Summary

**Background and Objective:** A precise identification of activated neurons facilitates understanding brain functions in physiology and diseases. We aimed at establishing a set of in situ hybridization probes of immediate early genes (IEGs) for mapping brain activity in mice with high spatial resolution.

**Methods:** First, we performed in situ hybridization to analyze mRNA expression of IEGs in the mouse brain after odorant exposure. We used wild type mice and the cyclic nucleotide-gated channel subunit A2 (*Cnga2*)-null mice since CNGA2 is a key component of the olfactory signal transduction pathway in the main olfactory system. Second, we performed unilateral optogenetic stimulation of the striatum in freely moving transgenic mice that expressed a channelrhodopsin-2 (ChR2) variant ChR2(C128S) in striatal medium spiny neurons (MSNs). To identify photoactivated neurons we then analyzed IEG expression patterns by in situ hybridization.

**Results and Discussions:** First, we observed rapid, robust and transient induction of as many as ten IEGs in the mouse olfactory bulb (OB) after odorant stimulation. In *Cnga2*-null mice, which are usually anosmic and sexually unresponsive, glomerular activation was insignificant as expected. However, a subtle induction of *c-fos* took place in a few mutants which exhibited sexual arousal. Interestingly, very strong glomerular activation was observed in mutants after exposure to a predator odor suggesting involvement of CNGA2-independent signaling pathways in the main olfactory system.

Second, we found that after in vivo unilateral photoactivation of the striatum induction of commonly used IEGs such as *c-fos*, *Arc* and *Egr1* was not apparent whereas *Npas4* was robustly induced in MSNs ipsilaterally.

**Conclusion:** Olfactory stimulation induced several IEGs in the mouse brain and the expression level corresponded well with the nature of the stimuli as well as interanimal behavioral differences. Using optogenetic manipulation we show that *Npas4* is a reliable marker of photoactivated MSNs. Together, our in situ hybridization probe set will be very useful to study brain activity at the cellular level in mice.

## List of reference articles

- ① Asim K Bepari, Keisuke Watanabe, Masahiro Yamaguchi, Nobuaki Tamamaki and Hirohide Takebayashi. Visualization of odor-induced neuronal activity by immediate early gene expression.  
**BMC Neuroscience** 13: 140, 2012 (IF= 3.0)
2. Asim K. Bepari, Hiromi Sano, Nobuaki Tamamaki, Atsushi Nambu, Kenji F. Tanaka, Hirohide Takebayashi. Identification of Optogenetically Activated Striatal Medium Spiny Neurons by *Npas4* Expression.  
**PLOS ONE** 7: e52783, 2012 (IF=4.1)
3. Hirohide Takebayashi, Masao Horie, Asim K Bepari, Keisuke Watanabe and Reiko Meguro. Strategy for Neuroscience Research Based on Neuroanatomy.  
**Niigata Medical Journal** (*in press*)

## Acknowledgments

I am highly thankful to Professor Nobuaki Tamamaki for his generous help throughout my doctoral study. Very often he used to enquire about the wellbeing of my study and my family and extend his kind supports whenever required.

One of my greatest treasures is to have Professor Hirohide Takebayashi, Division of Neurobiology and Anatomy, Graduate School of Medical and Dental Sciences, Niigata University, as my mentor. I gratefully acknowledge his kindness, guidance and supports throughout my doctoral study and stay in Japan. With every question, success and failure, I could reach him and was blessed with the best solution, appreciation and inspiration.

I am indebted to Dr. Keisuke Watanabe, now at Niigata University, for his very kind help for my research and my daily life. He taught me many experimental techniques very kindly, patiently and repeatedly.

I thankfully acknowledge the supports I received from my academic tutor Dr. Noriyoshi Usui starting from my very first days in Japan. He kindly taught me many research techniques.

I gratefully acknowledge Ms. Kanoko Nomura, then secretary at the Department of Morphological Neural Science, who is a friend of mine and my family, for her generous supports.

I am very much grateful to Dr. Masao Horie, Niigata University. With my many requests for my research and my family, he always extended his kind supports smilingly.

I am thankful to all lab members at the Department of Morphological Neural Science, Kumamoto University and the Division of Neurobiology and Anatomy, Niigata University for their support, guidance and encouragement to carry out my study.

We thank Dr. John Ngai, Dr. Nobuko Inoue and Dr. Hitoshi Sakano for *Cnga2*-null mice, Dr. Daniel Lévesque and Dr. Joseph Beavo for *Nor1* and *Pde2* plasmids, respectively and Ms. Mari Miyamoto and Dr. Yukiko Mori for excellent technical assistance. I am thankful to the animal facilities at Kumamoto University and Niigata University for maintaining the mouse colonies.

I am thankful to the Ministry of Education, Science, Sports and Culture of Japan (MEXT), the Global COE Program (Cell Fate Regulation Research and Education Unit), MEXT, Japan and Kumamoto University for financial supports.

I am grateful to all of my friends, well-wishers and relatives for their kind supports.

Words of thanks are never enough for what my parents and my sister are doing for me. In fact, they have made me what I am now. My wife's contributions for me are endless. Finally, I dedicate this thesis to my wife Bithi and my daughter Agnimitraa who inspire to live every moment with love and smiles.

## **List of abbreviations**

ACIII, Adenylyl cyclase type III

AOB, Accessory olfactory bulb

AON, Anterior olfactory nucleus

Cnga2, Cyclic nucleotide-gated channel subunit A2

EOG, Electro-olfactogram

G<sub>olf</sub>, Olfaction-specific G protein

IEG, Immediate early gene

ISH, In situ hybridization

MePD, Dorsomedial part of the medial amygdaloid nucleus

MOE, Main olfactory epithelium

MSN, Medium spiny neuron

OB, Olfactory bulb

OSN, Olfactory sensory neuron

PC, Piriform cortex

TMT, 2, 3, 5-trimethyl-3-thiazoline

## Background

The vertebrate brain has the enormous capability of responsiveness and adaptability with the diverse signals encountered in the environment. When an organism interacts with some sensory stimuli, the nervous system responds with activation of discrete neuronal ensembles. In many occasions, an altered environment triggers detectable behavioral responses. Consequently, analyses of the patterns of neuronal activation provide valuable insights into functions of different neuronal subgroups and brain regions for regulation of specific animal behaviors. Pioneering studies in 80's identified *c-fos* and several other genes, termed as immediate early genes (IEGs), which exhibited rapid and transient transcriptional activation when cells were stimulated in vitro (Cochran et al., 1983; Greenberg and Ziff, 1984; Sheng and Greenberg, 1990). Subsequent works revealed that in the nervous system a large number of genes show activity-dependent induction when neurons are stimulated by membrane depolarization, seizure or some sensory signals (Flavell and Greenberg, 2008; Leslie and Nedivi, 2011).

The neuronal IEGs comprise of several categories including transcription factors (*c-fos*, *Fosb*, *c-jun*, *Junb*, *Egr1*, *Egr2*, *Egr3*, *Npas4*, *Nr4a1*, *Nr4a2*, etc.) and postsynaptic proteins (*Arc*, *Homer1a*, etc.). Expression pattern of IEGs has emerged as a convenient tool for visualization of brain activities (Flavell and Greenberg, 2008; Okuno, 2011).

Among the IEGs *c-fos* is the most widely used activity marker and the studies of the *c-fos* mRNA expression or Fos-immunoreactivity contributed a lot in delineating the

signal processing in neuronal circuits which respond to various physiological, environmental and pharmacological stimuli (Hoffman and Lyo, 2002; Kovács, 2008). Nevertheless, previous studies indicated that *c-fos* is not a universal marker for neuronal activation and IEGs may be differentially induced depending on the neuronal population and/or the stimulus. For instance, Isogai et al. (2011) found that *Egr1*, but not *c-fos*, was induced robustly in mouse vomeronasal organ following sensory stimulation (Isogai et al., 2011). Although induction of c-Fos is widely used as an indication of striatal activation by several types of drugs of abuse in rodents (Nestler, 2001), an atypical antipsychotic drug clozapine was found to induce *Egr1* but not *c-fos* mRNAs in rat striatum (Nguyen et al., 1992). Therefore, accumulating evidence suggest that an enriched repertoire of neuronal activity-markers will foster studies involving brain mapping with a high spatial resolution. The objective of the present study was to compare inducibility of commonly used IEGs and to identify any other activity-dependent gene(s) which would be suitable for sensitive detection of change in neuronal activity. We performed in vivo stimulation in mice and then examined expression patterns of activity-dependent genes in the mouse brain by in situ hybridization (ISH).

**Part-I: Visualization of odor-induced neuronal activity  
by immediate early gene expression**

## **Introduction-I**

En route to the central nervous system sensory information occasionally follows polysynaptic pathways and displays substantial transfer across hemispheres. Transduced signals are processed in complex neuronal networks which are often dealing with other sensory modalities. This implies that although environmental changes almost invariably induce alteration in neuronal activity, it would be difficult to deduce a direct relationship between a stimulus and the observed brain activity at the cellular level. The olfactory system in mice represents several unique advantages in these regards. Olfactory sensory neurons (OSNs) synapse directly with second order neurons in the central nervous system and the projection is mostly ipsilateral.

In mammals each OSN usually expresses one of about 1000 olfactory receptors and in the olfactory epithelium OSNs are distributed randomly within distinct zones (Ressler et al., 1993; Vassar et al., 1993; Lin and Ngai, 1999). The sensory neurons extend a single axon to the olfactory bulb (OB) and the OSNs which express a particular olfactory receptor usually converge to a single glomerulus both in the medial and lateral halves of the OB (Ressler et al., 1994; Mombaerts et al., 1996; Wang et al., 1998). Therefore, OB glomeruli represent a topographical map of ORs in such a way that activation of distinct subsets of OSNs by a specific odorant is accompanied by activation of spatially segregated glomeruli in the OB (Wang et al., 1998; Mombaerts, 2006; Mori et al., 2006).

The olfaction-specific G protein (Golf) is activated when odorant molecules interacts with olfactory receptors on OSNs in the olfactory epithelium. Subsequently, other

components of the olfactory signaling cascades, the adenylyl cyclase type III (ACIII) and the olfactory cyclic nucleotide-gated channel (CNGC), are also stimulated (Kaupp, 2010).

Previous knockout mice studies have confirmed that the cAMP signaling pathway plays the key role for detection of odorants (Ronnelt and Moon, 2002; Spehr and Munger, 2009). Most of the Golf-deficient mice were found to die during the neonatal period and there was a severe reduction in odor-evoked electrical activity of the OSNs (Belluscio et al., 1998). The odorant-induced EOG response was found to be completely ablated and the odorant-dependent avoidance learning was impaired in ACIII mutant mice (Wong et al., 2000). The mice with a mutation in the cyclic nucleotide-gated channel subunit A2 (*Cnga2*) gene, which encodes the CNGA2 subunit essential for the functions of CNGC, also show general anosmia (Brunet et al., 1996). *Cnga2*-null male mice displayed deficits in mating and aggressive behaviors and the authors suggested that the MOE has an essential role in regulating these social behaviors (Mandiyan et al., 2005). However, Restrepo and colleagues (2004) showed that several odorants, including putative pheromones, were behaviorally detected by the *Cnga2*-null mice (Lin et al., 2004). Electrophysiological and immunohistochemical studies revealed that those odorants generated responses both in the OSN and the OB (Lin et al., 2004).

For detection of brain responses using neuronal activity markers 1) basal expression of the marker gene should be low and 2) activity-induced upregulation should be high, so that a change in expression level is easily detected. It is also helpful to

analyze several IEGs since the induction thresholds of IEGs vary depending on the IEG, the stimulus and the tissue. In this present study we first established a set of in situ hybridization probes of about 20 activity-dependent genes. Then, we analyzed expression patterns of the IEGs in the mouse brain using different odor stimuli and compared inducibility and sensitivity of these IEGs for detection of neuronal activity following in vivo olfactory stimulation. We then asked how disruption of the CNGA2-dependent signaling cascades in the olfactory pathway affects brain response using *Cnga2*-null male mice which show general anosmia and sexual deficits.

## **Method-I**

### **Mice**

Pregnant ICR mice were purchased from Japan SLC, Inc. *Cnga2* mutant mice (JAX Mice stock number 002905) originated from Dr. John Ngai lab (Brunet et al., 1996) were kindly provided by Dr. Hitoshi Sakano (Serizawa et al., 2006). The *Cnga2* gene is localized on X chromosome. Therefore, *Cnga2*-null male mice were obtained by crossing wild type male mice and heterozygous female mice. Most of the *Cnga2*-null mice die during early postnatal period and only a few rare survivors can grow until adulthood. At least three wild type mice and two *Cnga2*-null mice were analyzed for each condition. Wild type male littermates were used as controls of *Cnga2*-null mice. Animals were fed ad libitum and maintained under a 12:12-hour light/dark cycle. All measures were taken to minimize pain or discomfort to the mice. All animal procedures were carried out following the guidelines of Kumamoto University and Niigata University.

### **Odorant exposure**

A clean cage is prepared in which a 1.5-ml microcentrifuge tube is attached to one inner wall using adhesive tapes. First the mice were exposed to overhead airflow for two hours in the cage without food and water. Then an undiluted odorant was pipetted into the microcentrifuge tube in the cage. Following odorants were used: Amyl acetate/Pentyl acetate (60  $\mu$ l, Wako, Japan), Propionic acid (60  $\mu$ l, Sigma-

Aldrich) and 2, 3, 5-trimethyl-3-thiazoline (TMT) (30  $\mu$ l, Contech, Canada). If not mentioned otherwise, mice were exposed to the test odorant continuously for 30 minutes, anesthetized and perfused transcardially. For analyzing IEG induction a mouse was tested only once to avoid data confounding by learning.

### **Mating assay**

Male mice were separated from the litter at weaning and maintained with other male littermates (2 mice per cage). Mice were habituated in the test cage for two hours as described above. A wild type estrous female mouse was introduced in the test cage. Sexual behaviors (sniffing, mounting and intromission) of the male mouse were observed and the test mouse was anesthetized and perfused transcardially at the end of the 30-minute exposure. Sexual behaviors were considered to be present if the test mouse did mounting (attempted/successful) at least once during the 30-minute period.

### **TMT-induced avoidance test**

Mice were habituated for approximately 10 minutes in the test cage (30.5 x 20 x 13 cm, without food, water, and lid) followed by the 3-minute test period. A piece of filter paper (~2 cm x 2 cm) soaked with distilled water (control) or TMT was introduced at one end of the cage and behaviors were observed. Avoidance was quantified as the number of events of withdrawal (the mouse approaches the odorant

without contacting it, immediately withdrawing from it) and non-avoidance behavior was counted as the number of events of crouching over (the mouse investigates and crouches over the filter paper) (Capone et al., 2005). Three *Cnga2*-null male and 3 wild type littermate male mice were used for this test. The test was done twice with intervals of at least 3 days.

### **In situ hybridization (ISH)**

ISH was performed as described previously (Masahira et al., 2006). After perfusion fixation with 4% PFA in phosphate-buffered saline (PBS), mouse brains were fixed overnight in the same fixative solution at 4°C. Brains were then immersed in 20% Sucrose in PBS for cryoprotection. Samples were then frozen in OCT compound (Tissue-Tek) and stored at -80°C until use. Coronal tissue sections (20-µm) were cut in a cryostat. Samples were digested with Proteinase K (1 µg/ml) for 75 minutes and post-fixed in 4% PFA. After pre-hybridization, specimens were incubated overnight at 65°C with digoxigenin (DIG)-labeled riboprobes (Information on ISH probes is provided in Table 1). Following washes, blocking was done by 1% sheep serum, 1% bovine serum albumin (BSA) and 0.1% Triton X-100 in phosphate-buffered saline (PBS). Afterwards, samples were incubated overnight at 4°C with alkaline phosphatase-conjugated anti-DIG antibody (1:2000, Roche Diagnostics, Germany). Sections were washed in MABT (100 mM Maleic acid, 150 mM NaCl, 0.1% Tween 20) and then in alkaline phosphatase buffer (100 mM NaCl, 100 mM Tris-HCl, pH 9.5, 50 mM MgCl<sub>2</sub>, 0.1% Tween-20, 5 mM Levamisole). Tissue sections were

treated with NBT/BCIP (Roche) mixture at room temperature in dark for color development. After ISH staining, sections were counterstained by nuclear fast red.

**Table 1: Information on ISH probes**

<b>Gene symbol</b>	<b>Remarks (Genbank accession number)</b>	<b>Gene Name Synonyms</b>
<i>Arc</i>	(AF162777)	<b>activity regulated cytoskeletal-associated protein</b> Arc3.1
<i>c-fos</i>	EST clone (BC029814)	<b>FBJ osteosarcoma oncogene</b> Fos, cFos
<i>c-jun</i>	EST clone (BC094032)	<b>Jun oncogene</b> Jun, Junc
<i>Chat</i>	Ref. Dev Biol 293: 348-357, 2006. (NM_009891)	<b>choline acetyltransferase</b>
<i>Egr1</i>	EST clone (NM_007913)	<b>early growth response 1</b> Egr-1, Krox-1, Krox-24, Zif268
<i>Egr3</i>	(NM_018781)	<b>early growth response 3</b> Pilot
<i>Fosb</i>	(NM_008036)	<b>FBJ osteosarcoma oncogene B</b>
<i>GFP</i>	Used for detection of ChR2(C128S)-EYFP	<b>Green fluorescent protein</b>
<i>Jun-B</i>	EST clone (BC003790)	<b>Jun-B oncogene</b>
<i>Nor1</i>	A kind gift from Dr. Levesque, Faculté de Pharmacie, Université de Montréal Ref. J Pharmacol Exp Ther.313(1):460, 2005 (NM_015743)	<b>nuclear receptor subfamily 4, group A, member 3</b> Nr4a3, NOR-1
<i>Npas4</i>	(NM_153553)	<b>neuronal PAS domain protein 4</b> Nxf
<i>Nr4a1</i>	(NM_010444)	<b>nuclear receptor subfamily 4, group A, member 1</b> NGFI-B, Nur77
<i>Pde2 (Pde2a)</i>	A kind gift from Dr. Joseph Beavo, Dept. of Pharmacology, University of Washington Ref: PNAS 94: 3388-3395, 1997	<b>phosphodiesterase 2A, cGMP-stimulated</b>
<i>Pvalb</i>	Ref. Neurosci Res 63: 213-223, 2009. (NM_013645)	<b>Parvalbumin</b> Parv, PV, Pva
<i>Th</i>	(NM_009377.1)	<b>tyrosine hydroxylase</b>

### **Quantification of IEG expression**

Images of stained coronal sections of the OB were captured with an Olympus microscope and digital camera system (BX53 and DP72; Olympus, Tokyo, Japan). Quantification was performed using Adobe Photoshop CS5 Extended (version 12.0.4x64, Adobe Systems Incorporated) adapting the techniques described previously (Lehr et al., 1999; Mofidi et al., 2003). Signal intensity (arbitrary unit) of IEGs was calculated as the percentage of area positive for ISH signals in respective layers of the OB. Data were plotted in column charts where columns represented mean $\pm$  SEM. Seven to eight bulbs (approximately from + 4.5 mm bregma to + 4 mm bregma) from two to three mice were analyzed.

### **Statistical analysis**

Student's t-test was performed to compare means. Difference between groups was considered highly significant (\*\*) when  $p \leq 0.01$  and significant (\*) when  $p \leq 0.05$ .

## **Results-I**

### **Olfactory stimulation triggered rapid induction of ten activity-dependent genes in the mouse OB**

Mice are exposed to many odorants in their home cages in usual laboratory conditions. To reduce the level of ambient odorants mice were transferred to a clean

cage without bedding, food and water and were kept under overhead airflow for about two hours. The mice which were analyzed immediately after this habituation period were treated as the control group and termed as ‘Odorant (-)’. To activate the olfactory system we first used amyl acetate (AA) which is a standard nonbiological odorant. It is known that amyl acetate produces activation of a large number of OB glomeruli in rodents (Zhao et al., 1998; Rubin and Katz, 1999). To avoid habituation to the odorant we performed intermittent exposures, 5-minute exposures with 5-minute intervals, for 25 minutes. When the mice were analyzed after 30 minutes of the odor onset (AA 25 min, Air 5 min), we observed substantial increase in expression of as many as ten IEGs in the OB (**Figure 1.1A2-J2, A2’-J2’, Figure 1.2**) compared to the very low expression level of these genes in the control group (**Figure 1.1A1-J1, A1’-J1’, Figure 1.2**). We also checked IEG expression after 60 minutes of the onset of amyl acetate exposure (AA 25 min, air 35 min). There was a significant decline in mRNA expression of most of the IEGs (**Figure 1.1A3-J3, Figure 1.2**) although odorant-induced higher expression levels of *Egr3* (**Figure 1.1E1-E3**), *Fosb* (**Figure 1.1F1-F3**) and *Nor1* (**Figure 1.1H1-H3**) seemed to be sustained at least for 60 minutes from the initial odor presentation.

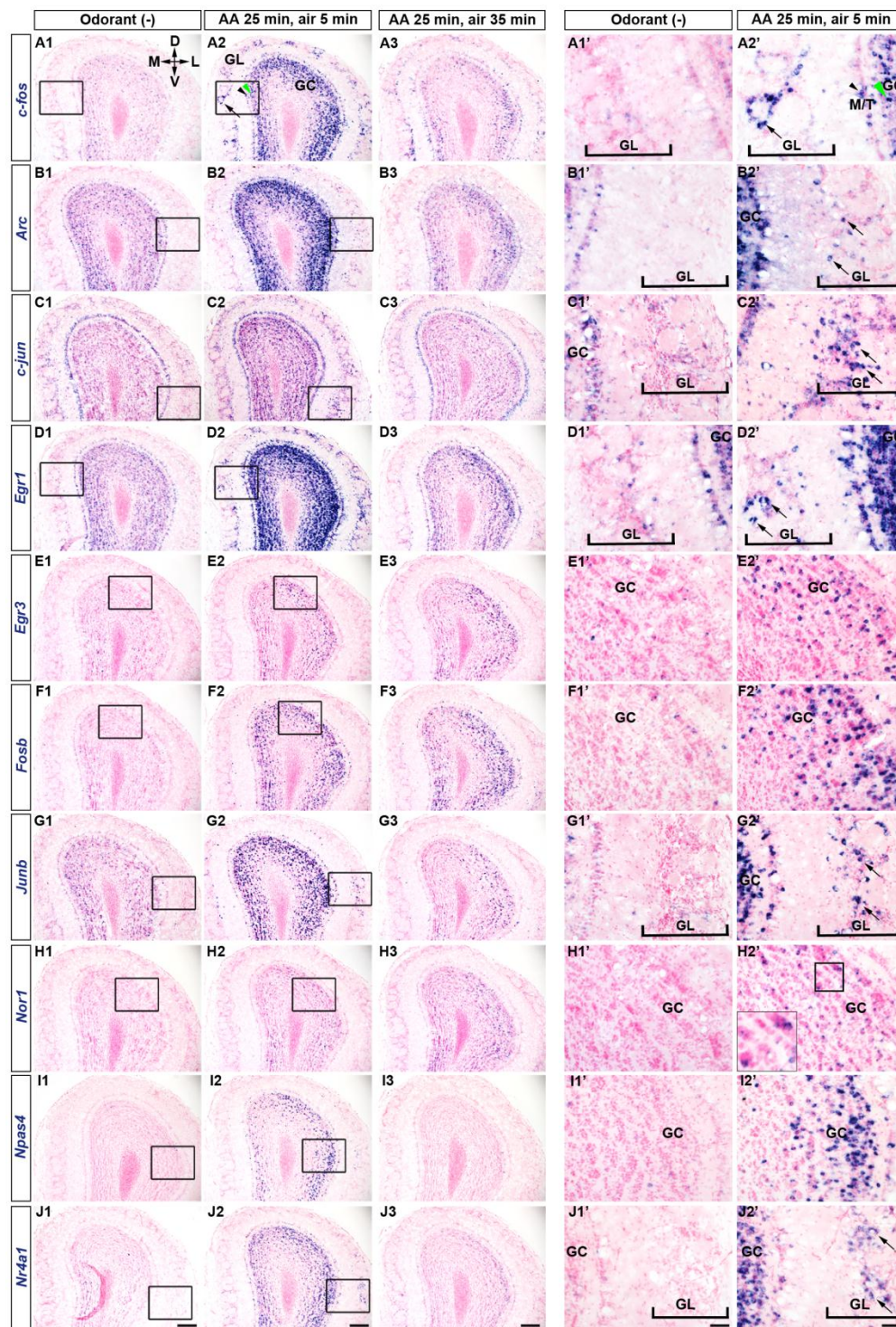


**Figure 1.1. Odorant (amyl acetate) exposure induced expression of IEGs in the mouse OB.** Mice were exposed to overhead airflow for two hours and then to the test

odorant (amyl acetate) for 25 minutes (5-minute exposures with 5-minute intervals). The ISH of coronal sections of OB indicated low expression levels of ten IEGs in mice after the 2-hour air exposure, (Odorant (-), A1-J1, A1'-J1'). All these ten IEGs were induced in the mouse after 30 minutes of odor onset (AA 25 min, air 5 min, A2-J2, A2'-J2'). Boxed areas in A1-J1 and A2-J2 are magnified in A1'-J1' and A2'-J2', respectively. Inset in H2' is a magnified view of the boxed area. Odor-evoked induction of IEG expression was transient and expression levels of most of the IEGs declined after 60 minutes of initial odorant exposure (AA 25 min, air 35 min, A3-J3). Arrows indicate GL, black arrowheads indicate M/T and green arrowheads indicate GC. AA-amyl acetate, GL-Glomerular layer, M/T-Mitral/Tufted cell layer, GC-Granule cell layer. D-Dorsal, V-Ventral, M-Medial, L-Lateral. Scale bar: (A1-J3) 200  $\mu$ m, (A1'-J2') 50  $\mu$ m

.....

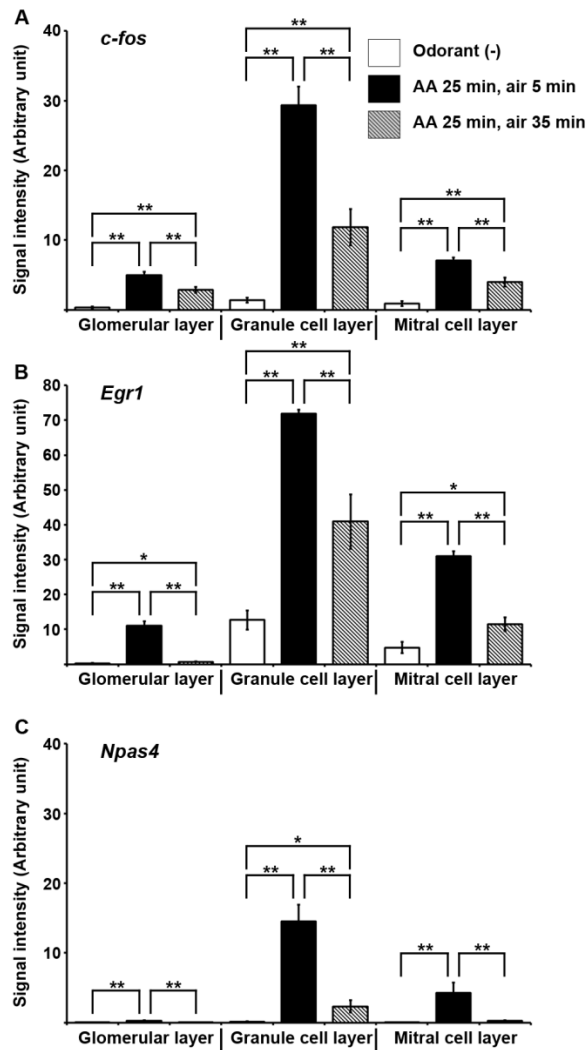


**Figure 1.2. Quantification of odor-evoked IEG induction in the mouse OB.**

Signal intensity (arbitrary unit) of IEGs (A. *c-fos*, B. *Egr1* and C. *Npas4*) was calculated as the percentage of area positive for ISH signals in respective layers of the OB. Columns represented mean  $\pm$  SEM. Seven to eight bulbs (approximately from + 4.5 mm bregma to + 4 mm bregma) from two to three mice were analyzed. Student's *t*-test was performed to compare means. \*\* Difference between groups was highly significant ( $p \leq 0.01$ ). \* Difference between groups was significant ( $p \leq 0.05$ ).

The main projection neurons in the mouse OB are the mitral/tufted cells and there are several types of interneurons such as granule cells and periglomerular cells. We could visualize activation of spatially segregated glomeruli by the strong *c-fos* expression in periglomerular cells (arrow, **Figure 1.1A2, A2'**) even though the ISH signals spanned the entire glomerular layer. The *c-fos* mRNA signals were abundant in the mitral/tufted cell layer (black arrowhead, **Figure 1.1A2, A2'**) and very dense signals were observed in the superficial aspects of the granule cell layer (green arrowhead, **Figure 1.1A2, A2'**). Similarly, we observed robust induction of *Arc*, *c-jun*, *Egr1* and *Junb* after the odorant exposure (**Figure 1.1**). It appeared that at the activated glomeruli *Egr1* induction took place in the majority of periglomerular cells (arrows, **Figure 1-1D2'**), whereas, *Arc*, *c-jun* and *Junb* were upregulated in subsets of periglomerular cells (arrows, **Figure 1-1B2', C2', G2'**, respectively).

In control mice signals of *Egr3*, *Fosb*, *Nor1*, *Npas4* and *Nr4a1* mRNAs were barely detectable either in the glomerular layer or in the mitral/tufted cell layer although a small fraction of granule cells were positive for these IEGs (**Figure 1.1E1, E1', F1, F1', H1, H1', I1, I1', J1, J1'**). After the amyl acetate exposure, significant induction of these five IEGs was apparent in the granule cell layer (**Figure 1.1E2, E2', F2, F2', H2, H2', I1, I1', J2, J2'**) and sparse signals appeared in a few periglomerular cells and the mitral/tufted cells (**Figure 1.1J2'**, data not shown).

In our subsequent experiments we analyzed induction patterns of *c-fos*, the most widely used IEG, along with *Npas4* since the activity-dependent induction of *Npas4* has not been previously reported in the mouse olfactory system. It was interesting to

note that after 30 minutes of odor onset, *Npas4* expression was robustly increased from a very low basal level and then, there was a steep decline within 60 minutes of odor onset (**Figure 1.1I1-I3**, **Figure 1.2C**). Our results indicated that expression patterns of IEGs in the mouse OB varied considerably at the basal condition and a single session of odorant exposure was sufficient to induce expression of the ten IEGs we examined.

### **Different odorants produce differential responses in the mouse brain**

The OB glomeruli are spatially organized into the dorsal (D<sub>I</sub> and D<sub>II</sub>) and the ventral (V) domains and different odorants activate distinct sets of glomeruli in the mouse OB (Mori and Sakano, 2011). Therefore, we used two different odorants for olfactory stimulation and then observed the neuronal activation pattern by ISH of activity-dependent genes. When we exposed mice to propionic acid, an aliphatic acid with pungent odor, we found that only a small number of glomeruli were strongly activated at the dorsomedial aspect of the anterior OB (arrowheads, **Figure 1.3A**, A') (Inaki et al., 2002; Matsumoto et al., 2010). There were strong signals of *c-fos* mRNAs in periglomerular cells around the glomeruli which were presumed to be specifically activated by propionic acid. In addition, the induced expression of *c-fos* was observed in the mitral/tufted cell layer and the granule cell layer below the activated glomeruli (**Figure 1.3A**). Using optical imaging a previous study also showed that propionic acid specifically activated the anteromedial domain of the mouse OB (Uchida et al., 2000). On the other hand, amyl acetate, a strong neutral

odorant, activates many glomeruli both in the dorsal and the ventral OB (Guthrie et al., 1993; Inaki et al., 2002; Johnson et al., 2004; Kobayakawa et al., 2007).

We also found that amyl acetate robustly induced *c-fos* expression in a large number of periglomerular cells, mitral/tufted cells and granule cells in both the dorsal and ventral aspects of OB (**Figure 1.3B**). Induction of *Npas4* was evident mainly in the granule cell layer of the OB for both propionic acid and amyl acetate (**Figure 1.3A', B'**). Accessory olfactory bulb (AOB) neurons were found to respond to the volatile, conspecific as well as allospecific odor cues (Xu et al., 2005; Ben-Shaul et al., 2010). Our results were in agreement with the emerging evidence for the overlapping functions of the mouse OB and the AOB in processing olfactory cues (Trinh and Storm, 2003; Keller et al., 2009). Using ISH of IEGs we found that odorants like amyl acetate and propionic acid, which are not pheromones, induced *c-fos* expression not only in the OB but also in the AOB (**Figure 1.3A, B, C, D**). Induced expressions of *Npas4* were evident in the OB (**Figure 1.3A', B'**) for both of these odorants although *Npas4* was only slightly induced in the AOB (**Figure 1.3C', D', insets**). Therefore, these data indicate that the IEG induction patterns we observed were odorant-specific and by tracing IEG expression using ISH, it is possible to demarcate brain activities with very high spatial resolution.

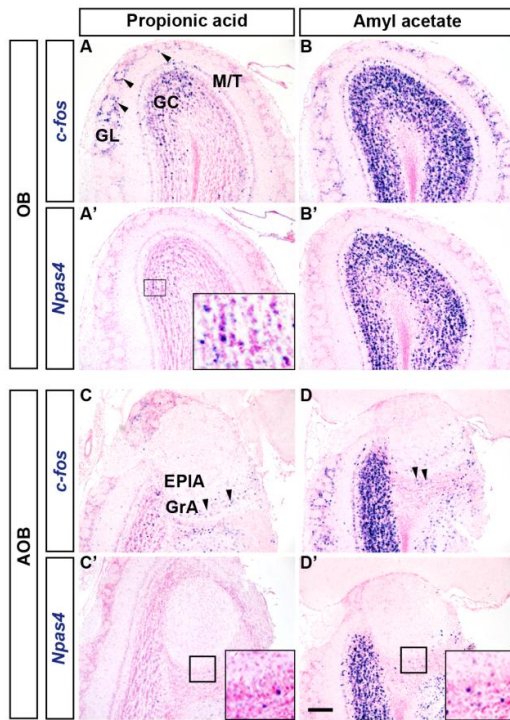


**Figure 1.3 Comparison of IEG induction patterns in response to two different odorants.** Mice were perfused transcardially after the 30-minute continuous exposure to the test odorant. (A, A') Propionic acid activated several glomeruli specifically in the dorsal OB (arrowheads in A). Induced expression of *Npas4* was observed only in the granule cell layer (A', inset). (B, B') A large number of glomeruli were activated by amyl acetate. *Npas4* induction was apparent only in the granule cell layer (B'). (C-D') Patterns of IEG induction in the AOB after odorant exposure. Arrowheads indicate *c-fos* induction in the granule cell layer of the AOB (C, D). Only a slight induction of *Npas4* was observed in the AOB (C'-D', insets). GL-Glomerular layer, M/T-Mitral/Tufted cell layer, GC-Granule cell layer, GrA-Granule cell layer of the AOB, EPIA- External plexiform layer of the AOB. Scale bar: 200  $\mu\text{m}$

## **IEG induction demarcates the flow of olfactory information in the higher order brain regions**

Olfactory information is conveyed to and processed in a number of cortical and subcortical brain regions including the anterior olfactory nucleus (AON), the piriform cortex (PC), the amygdala and the entorhinal cortex (Lledo et al., 2005; Castro, 2009).

We found that the increase in expression of these IEGs in AON (arrows, **Figure 1.4A-B'**) paralleled to the activation of OB neurons. It is known that in the PC pyramidal neurons receive direct input from mitral/tufted cells of the OB. Consequently, odorant exposure activates unique but overlapping subsets of neurons in the PC (Stettler and Axel, 2009). As expected, we observed odorant-induced increase in expression of IEGs in the layer 2/3 of the PC where cell bodies of pyramidal neurons are located (arrows, **Figure 1.4D, D'**).

Owing to the intimate connection between olfaction and memory, the hippocampus has been of great interest for studying olfactory memory. We found that the exploration of odor cues only for a brief period significantly induced the expression of several IEGs in the mouse hippocampus (**Figure 1.4E-F'**, data not shown). Our ISH data clearly indicate that odor stimulus not only triggered the robust induction of IEGs in the mouse OB but also conspicuously increased expression of these genes in various brain regions which are involved in olfactory signal processing.

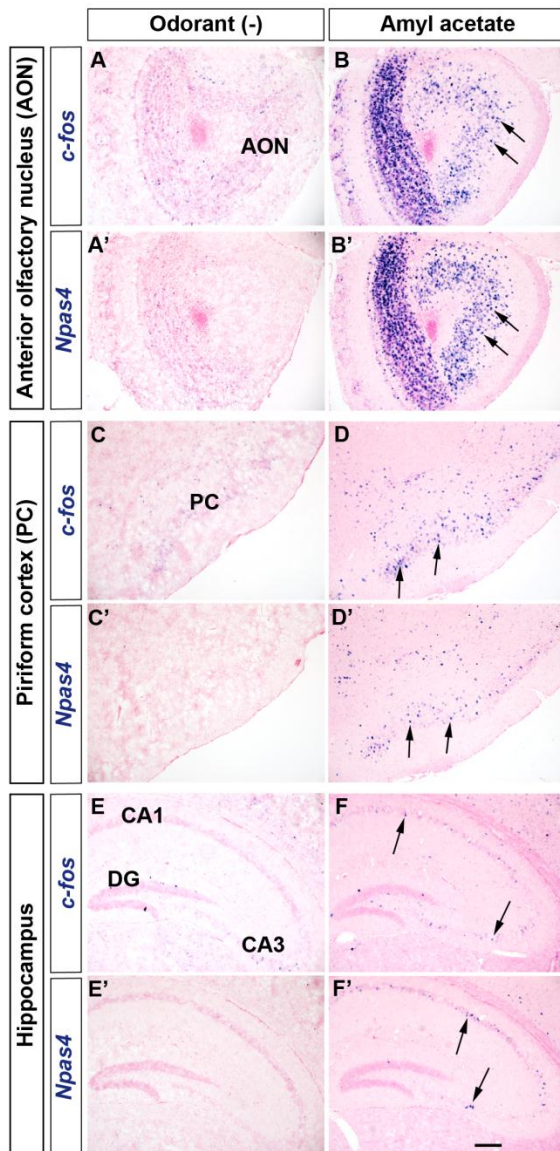


**Figure 1.4 Odorant exposure induced activity-dependent gene expression in different brain regions.** Odorant exposure induced expression of IEGs in the AON (arrows, A-B'), the PC (arrows, C-D') and the hippocampus (arrows, E-F'). Scale bar: 200  $\mu$ m

## **Individual differences in sexual stimuli-induced neuronal activities in *Cnga2*-null male mice**

It is interesting that most *Cnga2*-null male mice show neonatal mortality, general anosmia and deficits in sexual behaviors, however, a small number of the surviving male mutants can mate successfully (Brunet et al., 1996; Mandiyan et al., 2005). We tested the hypothesis whether the positive sexual behavior observed in some *Cnga2*-null male mice is correlated with a concurrent activation of the main olfactory system. In the home cage, mice experience many ambient odorants which are known to produce dense *c-fos* mRNA signals in olfactory structures (**Figure 1.5A1**) (Guthrie et al., 1993). First we checked the extent of IEG expression by such ambient odorants in the OB of male *Cnga2*-null mice. **Figure 1.5A** depicts a clear difference in *c-fos* expression patterns between mutant mice and their wild type littermates in home cages.

In the OB *c-fos* expression level was very low in mutants compared to that of wild type littermates (**Figure 1.5A1-A1'**). However, we observed strong *c-fos* signals in a few isolated glomeruli in the mutant OB (**Figure 1.6B3**). Expectedly, *c-fos* mRNA signals were practically absent in the AOB (**Figure 1.5A2-A2'**) in both the wild type and the mutant mice. Baker et al. (1999) and Lin et al. (2004) previously reported dramatically reduced tyrosine hydroxylase (TH) immunoreactivity, a marker for afferent activity, in most of the typical OB glomeruli in CNGA2-deficient mice (Baker et al., 1999; Lin et al., 2004).

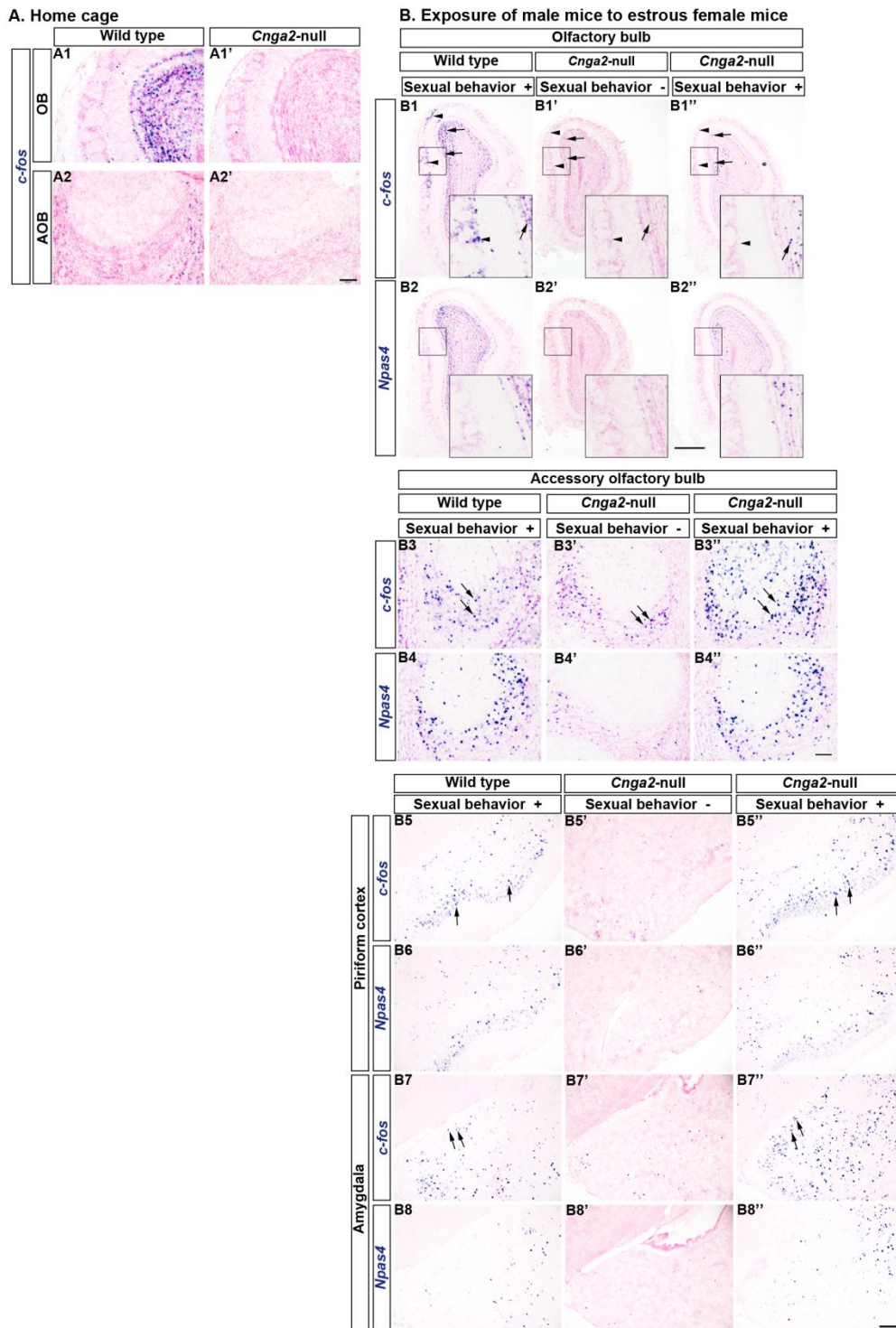


**Figure 1.5. Individual differences in induction of activity-dependent genes in *Cnga2*-null mice after exposure to female mice. A. Expression of *c-fos* in mice in**

their home cages without any odorant exposure. Significantly reduced expression levels of *c-fos* were observed in the OB (A1') and AOB (A2') of *Cnga2*-null male mice compared to that of wild type male littermates (A1, A2, respectively). B. Induction of *c-fos* expression in male mice which were exposed to estrous female mice. Arrowheads indicate the glomerular layer and arrows indicate the granule cell layer. Sexual stimulation by female mice induced expression of IEGs in the wild type OB (B1, B2). IEG induction was almost absent in the *Cnga2* mutants which did not show sexual behaviors (B1', B2'). IEG induction occurred in the OB, mainly in the granule cell layer, of the *Cnga2*-null male mice which showed sniffing and mounting behaviors (B1'', B2''). Insets in (B1-B2'') show magnified views of the boxed areas. IEG induction occurred in the AOB of male mice exposed to female mice (arrows, B3-B4''). (B5-B6'') Induction of IEGs in the PC (arrows) after exposure to female mice. Both in the wild type mice (B5, B6) and the mutants (B5'', B6'') which showed sexual behaviors, expression of IEGs was induced in the PC. IEG induction did not occur in the PC of *Cnga2*-null mice (B5', B6') which did not show sexual behaviors. (B7-B8'') Induction of IEGs in the MePD (arrows) after exposure to female mice. Both in the wild type mice (B7, B8) and the mutants (B7'', B8'') which showed sexual behaviors, expression of IEGs was induced in the MePD. The IEG induction did not occur in the MePD of *Cnga2*-null mice (B7', B8') which did not show sexual behaviors. Scale bars: (A1-A2' and B3-B4'') 100  $\mu\text{m}$ , (B1-B2'') 500  $\mu\text{m}$ , (B5-B8') 200  $\mu\text{m}$

.....

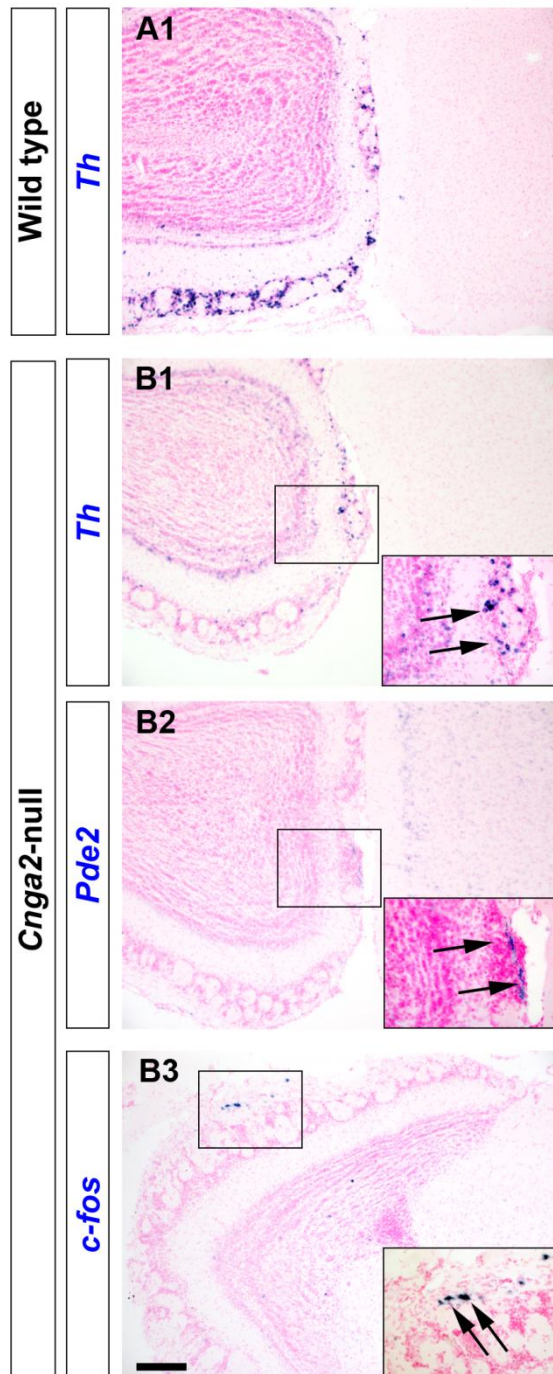


**Figure 1.6. Strong residual activity at the necklace glomeruli in *Cnga2*-null mice.** Figure shows horizontal sections of the OB. Expression of *Th*, a marker of afferent activity, was significantly reduced in most of the OB glomeruli in *Cnga2*-

null mice (B1) compared to that of wild type mice (A1). However, strong *Th* expression was observed in a small number of glomeruli (B1, inset), presumably the necklace glomeruli which express *Pde2* (B2, inset). In *Cnga2*-null mice *c-fos* expression was almost absent in the OB. However, strong *c-fos* signals appeared in a few glomeruli (B3, inset). Scale bar: 200  $\mu$ m.

.....

Nevertheless, in mutant mice strong TH staining was evident in a number of discrete glomeruli including the necklace glomeruli which are found at the posterior OB and are innervated by OSNs expressing a specific guanyl cyclase (GC-D) and a phosphodiesterase, PDE2 (Baker et al., 1999; Lin et al., 2004; Leinders-Zufall et al., 2007). In *Cnga2*-null mice we observed that *Th* mRNA expression was also significantly downregulated in most of the glomeruli while strong expression was retained only in a small number of glomeruli, presumably the necklace glomeruli (**Figure 1.6B1, B2**).

Since CNGA2 is expressed in almost all typical glomeruli, but not in necklace glomeruli which use cGMP as a second messenger instead of cAMP for olfactory signal transduction, our results supported the view that the cAMP pathway plays the key role for activation of the majority of ORNs and that olfaction is highly attenuated in the *Cnga2*-null mice (Brunet et al., 1996; Baker et al., 1999; Lin et al., 2004).

To check whether the main olfactory system in *Cnga2*-null male mice is unable to detect conspecific cues from female mice, we exposed *Cnga2*-null male mice and

wild type male littermates to estrous female mice. Wild type mice started chemoinvestigation (sniffing/licking) of the female anogenital regions almost instantly and did mounting (attempted or successful) within the first 3 minutes of exposure. As reported in a previous study (Mandiyan et al., 2005), the lack of sexual behaviors was clearly apparent in *Cnga2*-null male mice. Most of the *Cnga2*-mutant mice (7 out of 9 mice) did not initiate the exploration of female anogenital or facial regions. Instead, mutant male mice exhibited only occasional sniff-like behaviors often resembling grooming behaviors. We did not observe any mounting behavior in the *Cnga2*- null male mice during presentation of female mice for 30 minutes (data not shown). Nonetheless, sniffing/sniff-like behavior was observed within the first 3 minutes of exposure both in wild type mice and *Cnga2*-null mice. Neuronal activation in the OB was strikingly lower in those mutant mice (**Figure 1.5B1'**, **B2'**) compared to wild type male littermates (**Figure 1.5B1**, **B2**). Interestingly, a few (2 out of 9) *Cnga2*-null male mice showed positive sexual behaviors which were practically indistinguishable from the wild type behaviors. Those mutants started chemoinvestigation (sniffing/licking) of the female anogenital areas almost instantly and showed mounting behaviors even within the first minute of exposure. Despite the arousal of sexual behaviors the strong glomerular activation observed in the OB of wild type mice (arrowheads, **Figure 1.5B1**) was absent in those mutants. Interestingly, *c-fos* and other IEGs were induced in a small fraction of OB granule cells in the mutant mice (arrows, **Figure 1.5B1''**, **B2''**); although the induction was noticeably lower than that in wild type mice (arrows, **Figure 1.5B1**, **B2**).

Conspecific odor cues considerably induced expression of IEGs in the mouse AOB (arrows, **Figure 1.5B3, B4**, compare **Figure 1.5A2**). Even in the *Cnga2*-null male mice, a substantial IEG induction was observed in the AOB after exposure to the female stimuli (arrows, **Figure 1.5B3''**, **B4''**). Consistently, IEG induction was lower in the mutants which did not show any apparent sexual behavior (arrows, **Figure 1.5B3-B4''**).

We further analyzed neuronal activation in other brain regions of the *Cnga2*-null male mice which were exposed to female mice (**Figure 1.5B5-B8''**). We found that induction of *c-fos* expression was very low in the PC of the *Cnga2*-null mice which did not show sexual behaviors (arrows, **Figure 1.5B5'**, **B6''**). In rodents, exposure to estrous odors increased Fos immunoreactivity in the medial amygdala (Kippin et al., 2003) and this brain region was found to regulate attraction to female odor cues (Dhungel et al., 2011). We found that both in wild type mice and *Cnga2* mutants which displayed sexual arousal, a conspicuous induction of IEGs occurred in the posterodorsal part of the medial amygdaloid nucleus (MePD) (arrows, **Figure 1.5B7, B8, B7''**, **B8''**). Expectedly, the IEG induction in the MePD was much lower in the *Cnga2*-null male mice which did not show sexual behaviors (arrows, **Figure 1.5B7'**, **B8''**). These results provide the evidence that tracing IEG induction by ISH can detect differences in brain activities, with high spatial sensitivity, which correspond to individual behavioral differences. These results also indicate that the lack of amygdaloid activation following presentation of the female sexual stimuli may

contribute to the diminished sexual behaviors observed in the majority of *Cnga2*-null male mice.

### **TMT exposure activates the OB in *Cnga2*-null mice without eliciting avoidance**

We then sought to know if a strong odorant, amyl acetate, can trigger glomerular activation in the *Cnga2*-null OB in our experimental conditions. To our surprise, we observed robust activation of a large number of glomeruli by the emergence of dense *c-fos* mRNA signals in periglomerular cells and in the mitral/tufted cell layer and the granule cell layer below the activated glomeruli (**Figure 1.7A**). Interestingly, *c-fos* induction was stronger in the mutant OB, predominantly in the ventrolateral aspects, compared to that in the wild type OB (**Figure 1.7A**).

We next exposed the *Cnga2*-null mice and wild type littermates to the predator odor TMT which produces avoidance behaviors in rodents (Takahashi et al., 2005). For behavioral analyses we introduced a piece of filter paper soaked with distilled water or TMT in the mouse cage and observed avoidance behaviors such as stretch attend posture (the animal approaches and sniffs the filter paper with flat back and stretch neck) and withdrawal (the mouse approaches without contact and immediately withdraws from the stimulus) and non-avoidance behaviors such as crouching over object and catching (the mouse takes the filter paper in its mouth) (Capone et al., 2005). TMT-induced avoidance behaviors, as quantified by the events of withdrawal, were present in wild type mice but practically absent in *Cnga2*-null mice (**Figure**

1.7B1). In contrast, *Cnga2*-null mice showed non-avoidance behaviors including increased investigation and crouching over the TMT-soaked filter paper unlike their wild type littermates (**Figure 1.7B1**). We then checked IEG expression levels in the mice which were exposed to TMT for 30 minutes. TMT strongly induced *c-fos* mRNA expression in the wild type OB (**Figure 1.7B2**). Notably, we also observed strong induction of IEGs in the OB and the AOB of *Cnga2*-null mice (**Figure 1.7B2', B3'**, respectively) despite the absence of predator odor-induced avoidance response (**Figure 1-7B1**). Taken together, our results suggest that the predator odor TMT can strongly activate the main olfactory system in *Cnga2*-null mice although such activation seemed to fail to produce typical avoidance response.

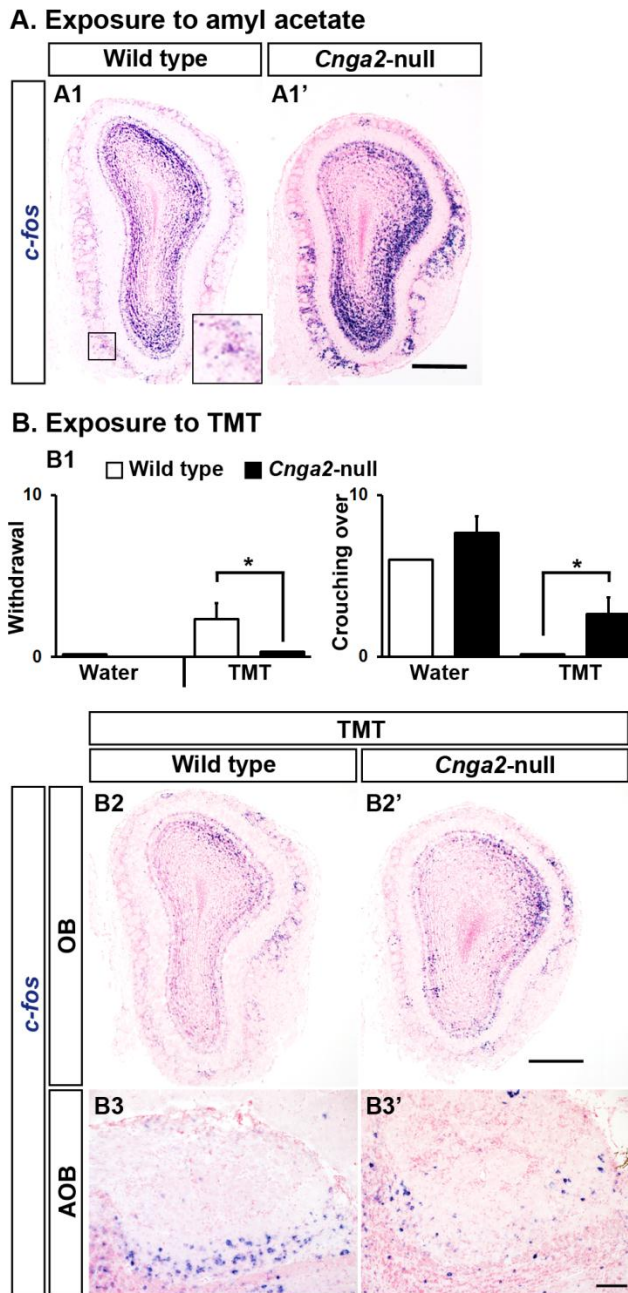


**Figure 1.7. Neuronal activation in response to amyl acetate and TMT in *Cnga2*-null mice.** A. A neutral odorant, amyl acetate, robustly induced *c-fos* expression in the OB in both wild type (A1) and *Cnga2*-null (A1') mice. Inset in A1 shows magnified view of the boxed area. B. Responses of mice after presentation of TMT, a

predator odor from fox. TMT-induced avoidance behaviors were present in wild type mice but absent in *Cnga2*-null mice (number of withdrawal, B1 left). Unlike wild type mice, *Cnga2*-null mice showed increased investigating behaviors for TMT (number of crouching over, B1 right). After exposure to TMT for 30 minutes, expression of *c-fos* was induced in both wild type and *Cnga2*-null mice in the OB (B2, B2', respectively) and the AOB (B3, B3', respectively). Scale bars: (A1, A1', B2, B2') 500  $\mu\text{m}$ , (B3-B3') 100  $\mu\text{m}$ .

.....

## Discussion-I

### Detection of neuronal activity using ISH of IEGs

Tracing IEG expression has been proved to be a very reliable and powerful tool for visualization of neuronal activities. In this study we compared mRNA expression patterns of ten IEGs using the ISH method. We found that these IEGs, which included both the transcription factors and effectors, were expressed at low levels in different brain regions in mice at the basal condition (**Figure 1.1-1.4**). We observed differential expression patterns of these activity-dependent genes in different cell layers of the mouse OB. Interestingly, all these genes were induced significantly in the OB after exposure of the mouse to a given odorant, presumably due to stimulation of the olfactory sensory pathway. However, an increasing number of studies indicate that centrifugal innervation can substantially modulate odor processing in the OB (Sallaz and Jourdan, 1996; Gómez et al., 2005; Kiselycznyk et al., 2006; Matsutani and Yamamoto, 2008). We observed IEG induction in spatially restricted regions in response to propionic acid whereas amyl acetate triggered global induction in the OB (**Figure 1.1, 1.2 and 1.3**). Therefore, we cannot rule out the possibility that central inputs had role in activation of a large number of OB granule cells we observed in some cases, for instance, after amyl acetate exposure.

The basic helix-loop-helix (bHLH)-PAS transcription factor *Npas4* has been previously identified as a critical factor in regulation of inhibitory synapse development on excitatory neurons (Lin et al., 2008) and recent reports indicate that the *Npas4* gene is involved in learning and memory (Yun et al., 2010; Ploski et al.,

2011). Expression of *Npas4* mRNA was found to be increased by membrane depolarization in vitro and by 1 hour light stimulation in vivo in the visual cortex of dark-reared mice (Lin et al., 2008). Our in vivo results indicate that the basal expression of *Npas4* is very low in the mouse OB and a brief olfactory stimulation is sufficient to induce this gene rapidly and transiently in the mouse brain (**Figure 1.111-12**, **Figure 1.2**).

We found that induction of both *c-fos* and *Egr1* took place in a greater number of cells in the OB compared to that of other IEGs, although the basal expression of *Egr1* was slightly higher (**Figure 1.2A1-A2**, D1-D2'). The rapid induction and the wider coverage of *c-fos* expression in different subtypes of cells explain the versatile use of *c-fos* in IEG mapping. Nevertheless, a different IEG may be suitable in a particular experimental setup depending on the neuronal cell type or the stimuli under consideration. For instance, in a recent study Isogai et al. (2011) compared the expression of several IEGs in the mouse vomeronasal organ and found that *Egr1*, but not *c-fos*, was induced robustly following sensory stimulation (Isogai et al., 2011). Likewise, our results suggest that *Npas4* would be a suitable marker to detect activated granule cells in the mouse OB.

### **Sexual behaviors in *Cnga2*-null male mice**

Previous studies indicated that inactivation of the main olfactory system considerably affects sexual behaviors in male mice (Keller et al., 2009). This view has been

substantiated by the observation of significant deficits in sexual behavior in male *Cnga2*-null mice (Mandiyani et al., 2005) since CNGA2 is essential for signal transduction in most of the MOE neurons (Dhallan et al., 1990; Waldeck et al., 2009; Kaupp, 2010). Consistently, we observed that in *Cnga2*-null male mice female sexual stimuli failed to activate the OB and did not initiate sexual behaviors although the IEGs were significantly induced in the AOB. However, there are individual differences and in a longer mating assay Shah and colleagues (2005) found that a female mouse cohabitating with mutants was plugged once and gave birth (Mandiyani et al., 2005). We also observed significant sexual arousal in a few *Cnga2*-mutant male mice (see results). This raised the possibility that a CNGA2-independent signaling pathway(s) can activate the OB to initiate sexual behaviors. Our study supports this idea, although it contradicts with the suggestion made by Mandiyani et al. (2005) that the sub-population of MOE neurons which use alternative signaling pathway cannot initiate mating responses (Mandiyani et al., 2005). We observed induction of IEGs in a significant number of OB granule cells and mitral/tufted cells in the *Cnga2*-null mice which initiated mating behaviors when exposed to estrous female mice (**Figure 1.5B1''**, B2''). Previously it has been suggested that the transient receptor potential channel M5 (TRPM5)-expressing OSNs which project to the ventral OB are involved in pheromone signaling in CNGA2-defective mice (Lin et al., 2007). In the *Cnga2* mutants we observed stronger induction of IEGs in the dorsal OB (arrows, **Figure 1.5B1''**, B2'') in addition to the weaker ventral induction. Therefore, another set of OSNs targeting glomeruli in the dorsal OB may participate

in transmitting olfactory signals sufficient to initiate mating behaviors in CNGA2-deficient mice. However, we cannot rule out the possibility that the sexual arousal observed in a few *Cnga2*-null male mice might have been initially triggered by sensory modalities other than olfaction, for instance, visual and/or auditory stimuli, which activated centrifugal inputs to the OB and induced IEGs predominantly in the granule cell layer (**Figure 1.5B1''-B2''**) secondary to the activation of the accessory olfactory system (**Figure 1.5B3''-B4''**).

#### **Strong glomerular activation in the OB of anosmic *Cnga2*-null mice**

Using ISH we compared the expression level of IEGs in the olfactory system of *Cnga2*-null mice and wild type control mice. We found that the environmental olfactory stimuli in usual laboratory conditions produce significant neuronal activities in the OB of wild type mice whereas the IEG expression levels were remarkably lower in the OB of *Cnga2*-null mice (**Figure 1.5A**).

Previously Lin et al. (2004) found that CNGA2-deficient mice detected some odorants and the authors suggested cAMP-independent pathways for the observed responses (Lin et al., 2004). Later, Munger and colleagues demonstrated that GC-D neurons, which lack CNGA2 and several other components of the canonical odor transduction pathway and axons of which innervate the necklace glomeruli, can utilize a cGMP-dependent signaling cascade for chemosensory transduction (Leinders-Zufall et al., 2007). In those previous studies only a small subset of

glomeruli including the necklace glomeruli were found to be activated by the suggested CNGA2-independent signaling pathway(s) (Lin et al., 2004; Leinders-Zufall et al., 2007). In contrast, we observed that amyl acetate robustly induced *c-fos* mRNA expression in the OB of *Cnga2*-null mice, notably at the ventrolateral OB, in a large number of glomeruli which could include, but apparently not limited to, the necklace glomeruli (**Figure 1.7A1'**). We also observed that TMT, a predator odor which produces fear responses in wild type mice, induced the expression of IEGs very strongly in the OB (**Figure 1.7B2'**) without eliciting any obvious fear response in *Cnga2*-null mice. Previously Kobayakawa et al.(2007) found that the mice in which the OSNs were ablated specifically in the dorsal olfactory epithelium lacked innate fear response to TMT even though the mice could detect the odorant (Kobayakawa et al., 2007). They proposed the existence of hard-wired circuits in the mammalian olfactory system for processing innate responses (Kobayakawa et al., 2007; Sakano, 2010). Our results indicate that a CNGA2-dependent signaling pathway may be essential for the mouse olfactory circuits to initiate innate fear responses.

In our experiments odorant concentrations were high since pure liquid odorants were introduced in the mouse cage. Previously it has been suggested that a cAMP-independent pathway(s) contributed in the EOG responses observed in the MOE of *Cnga2*-null mice exposed to odorants at relatively higher concentrations (Lin et al., 2004). Olfactory neurons expressing TRPM5 can detect the chemicals involved in animal communication and TRPM5-expressing OSNs project mainly to the ventral

OB (Lin et al., 2007). Indeed, we observed strong *c-fos* induction in a large number of glomeruli mainly in the ventral OB in *Cnga2*-null mice exposed to amyl acetate (**Figure 1.7A'**). In addition, a predator odor TMT strongly activated spatially segregated glomeruli in mutants (**Figure 1.7B2'**). However, along with direct peripheral inputs via OSNs, there could be other possibilities which might contribute to the odor-induced glomerular activation observed in *Cnga2*-null mice. Centrifugal inputs are known to modulate neuronal activities in the rodent OB, predominantly in the granule cell layer (Sallaz and Jourdan, 1996; Gómez et al., 2005; Kiselycznyk et al., 2006; Matsutani and Yamamoto, 2008) and might have contributed in the odorant-induced IEG inductions observed in the present study. Although *Cnga2*-null mice appeared normal in several behavioral tests including grooming (Restrepo et al., 2004; Mandiyan et al., 2005), the size of the OB is apparently smaller in the mutants and alteration in brain development has been suggested (Baker et al., 1999). Previous studies reported collateral innervation of the olfactory epithelium and OB by some trigeminal ganglion cells in rats (Schaefer et al., 2002; Brand, 2006). Trigeminal activation was found to inhibit olfactory responses (Kratskin et al., 2000; Brand, 2006) and thus, the role of trigeminal activation might be insignificant for IEG induction in our experiments. It was interesting that amyl acetate-induced *c-fos* expression was stronger in *CNGA2*-deficient mice compared to wild type mice and may suggest impaired peripheral adaptation in glomeruli (Lecoq et al., 2009) and/or reduced presynaptic inhibition of OSNs (Pírez and Wachowiak, 2008) in mutants although further studies will be needed to decode the observed phenomena.

However, without the CNGA2 subunit there is no functional CNG channel for transduction of olfactory signals in most of the MOE neurons (Dhallan et al., 1990; Waldeck et al., 2009). Together, our data provide support for the idea that in addition to the CNGA2-dependent pathway other alternative signaling pathways participate in signal transduction in the mouse main olfactory system.

**Part-II: Identification of optogenetically activated  
striatal medium spiny neurons by *Npas4* expression**

## **Introduction-II**

Optogenetics is a powerful neuromodulatory tool with many unique advantages to explore functions of neuronal circuits in physiology and diseases (Yizhar et al., 2011). Incorporation of microbial light-activated channel proteins in experimental animals allows manipulation of electrical activity of the target tissue with the millisecond temporal precision even in freely moving animals. When functional light-activated channel proteins are expressed in neurons both gain-of-function and loss-of-function studies are possible to modulate animal behaviors and to infer causal relationship between the illuminated neurons and the resultant cellular or behavioral changes in physiological or pathophysiological conditions. For instance, Brown et al. (2010) found that direct optical activation of dopamine (DA) neurons of the mouse ventral tegmental area (VTA) was sufficient to drive redistribution of AMPA receptors (Brown et al., 2010). Deisseroth and colleagues demonstrated that selective high-frequency stimulation of afferent axons projecting to the subthalamic nucleus robustly ameliorated the disease symptoms in a rodent model of Parkinson's disease (PD) (Gradinaru et al., 2009).

Interpretation of cellular and behavioral responses following in vivo optogenetic manipulation of brain activities in experimental animals often necessitates identification of photoactivated neurons with high spatial resolution. Very often, this is a challenging task since the illuminated cells are inevitably heterogeneous in terms of intensity of the incident light (Yizhar et al., 2011). This limitation calls for additional measures for sensitive detection of photoactivated cells with high spatial

resolution. One convenient approach is the visualization of activated neurons by tracing induction of immediate early genes (IEGs) such as *c-fos*, *Egr1* and *Arc* (Schoenenberger et al., 2009; Covington et al., 2010; Wen et al., 2010; Lin et al., 2011).

Nevertheless, previous studies indicated that *c-fos*, the most widely used IEG, is not a universal marker for neuronal activation and IEGs may be differentially induced depending on the neuronal population and/or the stimulus. For instance, Isogai et al. (2011) found that *Egr1*, but not *c-fos*, was induced robustly in the mouse vomeronasal organ following sensory stimulation (Isogai et al., 2011). Though several types of drugs of abuse can induce *c-fos* in the striatum (Graybiel et al., 1990; Nestler, 2001), an atypical antipsychotic drug clozapine was found to induce *Egr1* but not *c-fos* mRNAs in the rat striatum (Nguyen et al., 1992). Using in vivo light stimulation followed by in situ hybridization of activity markers here we show that the neuronal IEG *Npas4* can identify photoactivation of striatal MSNs more reliably compared to other commonly used IEGs like *c-fos*, *Egr1* and *Arc*.

## **Method-II**

### **Mice**

PDE10A2-tTA mice were obtained from RIKEN BRC Bank (RBRC No. RBRC02317, Strain B6.129-Pde10a2<tm1(tTA)Yok>) (Sano and Yokoi, 2007). The tetO-ChR2(C128S)-EYFP BAC transgenic mice were crossed to PDE10A2-tTA mice to generate compound heterozygous mice (Tanaka et al., 2012). Animals were kept under regulated air conditions ( $23\text{ }^{\circ}\text{C} \pm 1\text{ }^{\circ}\text{C}$ ) and a 12:12 hours light-dark cycle throughout the experiments. Food and water were available ad libitum. Two to three mice were analyzed for each condition. All animal procedures were approved by the Animal Research Committees of the National Institute for Physiological Sciences, Keio University and Niigata University.

### **In vivo optical stimulation and electrophysiological recording of striatal neurons**

To fix the head of the awake mouse in a stereotaxic apparatus, a small U-frame head holder was mounted on the head as reported previously (Chiken et al., 2008). Each mouse was anesthetized with ketamine hydrochloride (100 mg/kg body weight, i.p.) and xylazine hydrochloride (5 mg/kg body weight, i.p.) and fixed in a conventional stereotaxic apparatus (Narishige Scientific Instrument, Tokyo, Japan). The skull was widely exposed, and periosteum and blood on the skull were removed completely. The exposed skull was completely covered with bone adhesive resin (BISTITE II, Tokuyama, Tokyo, Japan) and acrylic resin (UNIFAST II, GC Corporation, Tokyo,

Japan), and then a small U-frame head holder was mounted and fixed with acrylic resin on the head of the mouse. After recovery from the first surgery (2 or 3 days later), the mouse was positioned in a stereotaxic apparatus with its head restrained using the U-frame head holder under light anesthesia with ketamine hydrochloride (50-100 mg/kg body weight, i.p.). A part of the skull in one hemisphere was removed to access the striatum.

After full recovery from the second surgery, the mouse was positioned in a stereotaxic apparatus with its head restrained using a U-frame head holder in the awake condition. For recording neural activity while illuminating with blue light, an electrode assembly consisting of a glass-coated Elgiloy microelectrode (0.5-1.0 M $\Omega$  at 1 kHz) and a 50  $\mu$ m diameter optical fiber (CeramOptec Industries, East Longmeadow, MA, USA), was inserted perpendicularly into the brain through the dura mater using a hydraulic microdrive (Narishige Scientific Instrument, Tokyo, Japan). A blue laser (50 mW, CrystaLaser, Reno, NV, USA) was coupled to the optical fiber. The laser power was  $\approx$  40 mW at the fiber tip. The laser was controlled via TTL pulses driven by a stimulator (Nihon Kohden, Tokyo, Japan). The target area was 0.0-0.5 mm anterior and 2.0-2.2 mm lateral to bregma and 2.5-4.0 mm deep from the brain surface for the striatum (Franklin and Paxinos, 2007). Signals from the electrode were amplified, filtered (0.3-10 kHz), and sampled at 50 kHz using a computer.

### **In vivo optical stimulation in freely moving mice**

Each mouse was anesthetized with ketamine hydrochloride and xylazine hydrochloride and fixed in a conventional stereotaxic apparatus (David Kopf, CA, USA). A plastic optical fiber (ESKA, Mitsubishi Rayon, Tokyo, Japan, 0.5 mm diameter) was inserted in each cerebral hemisphere above the dorsal striatum. The tip of the fiber located approximately at 0.7 mm posterior and 2.0 mm lateral to bregma, and 2.0 mm deep from the skull. The fiber was fixed on the skull using Aron Alpha (Toagosei Co., LTD., Tokyo, Japan). The mice were allowed to recover for at least one week after fiber implantation. For optical stimulation of striatal neurons, a single 500-ms illumination ( $6.7 \text{ mW/mm}^2$  at the fiber tip) was given to the left striatum in the home cage. No optical stimulation was given to the right striatum and this served as the sham-treated control. Mice were anesthetized with ketamine hydrochloride and xylazine hydrochloride after 5 minutes of optical stimulation and perfused transcardially after additional 5 minutes.

### **In situ hybridization**

*In situ* hybridization was performed as described previously (Usui et al., 2012) using DIG-labeled riboprobes (Table 1). Briefly, 20- $\mu\text{m}$  sections were prepared from frozen mouse brain samples. Sections were fixed in 4% PFA, digested with Proteinase K (1  $\mu\text{g/ml}$ ), acetylated and then hybridized with DIG-labeled riboprobes overnight at 65°C. DIG-labeled RNA hybrids were reacted with an alkaline

phosphatase-conjugated anti-DIG antibody (1:2000, Roche) overnight at 4°C. Sections were washed in MABT (100 mM Maleic acid, 150 mM NaCl, 0.1% Tween 20) and then in alkaline phosphatase buffer (100 mM NaCl, 100 mM Tris-HCl, pH 9.5, 50 mM MgCl<sub>2</sub>, 0.1% Tween 20, 5 mM Levamisole). Tissue sections were treated with NBT/BCIP (Roche) mixture at room temperature in dark for color development. After ISH staining, sections were counterstained by nuclear fast red.

### **Double fluorescent in situ hybridization (Double FISH)**

Procedures for double FISH were adopted from a previous study (Tanaka et al., 2012). In brief, frozen tissue sections were hybridized with FITC-labeled *Npas4* cRNA probe and DIG-labeled *GFP*, *Chat* or *Pvalb* cRNA probes. After stringent washing sections were incubated with a peroxidase-conjugated anti-FITC antibody (Roche, 1:200, 30 minutes at room temperature) and signals were visualized by FITC (TSA Plus Cyanine 3/Fluorescein System, PerkinElmer, Foster city, CA). Residual peroxidase activity was quenched by 2% H<sub>2</sub>O<sub>2</sub> (30 minutes at room temperature). Samples were then incubated with a peroxidase-conjugated anti-DIG antibody (Roche, 1:200, 60 minutes at room temperature) and signals were visualized by Cy3 (TSA Plus Cyanine 3/Fluorescein System, PerkinElmer). Confocal fluorescence images were captured using a laser scanning microscope system (LSM 710, Carl Zeiss Microimaging, Germany). It should be noted that in the standard chromogenic *Npas4* ISH, we usually observed weaker perinuclear signals and stronger nucleolar

signals. In Double FISH using TSA amplification system, we mostly observed strong dot-like *Npas4* signals.

### **Quantification of ISH signals**

Images of stained coronal sections of the mouse brain were captured with an Olympus microscope (BX53, Olympus, Tokyo, Japan) and digital camera system (DP72, Olympus). The cells which were positive for ISH signals were counted in the dorsolateral striatum from five coronal tissue sections (approximately  $\pm 0.5$  mm bregma) from one representative animal. Student's t-test was performed to compare means. Difference between groups was considered highly significant when  $p \leq 0.01$  and significant when  $p \leq 0.05$ .

## **Results-II**

### **In vivo optical stimulation of striatal MSNs**

To drive cell type-specific expression of a highly light-gated channelrhodopsin-2 (ChR2) variant ChR2(C128S) (Berndt et al., 2008) we took advantage of the tetracycline-controlled transcriptional activator (tTA) system. Previously it was demonstrated that tTA is stably expressed in almost all striatal MSNs of PDE10A2-tTA mice (Sano and Yokoi, 2007). Recently the tetO-ChR2(C128S)-EYFP BAC transgenic mouse line has been established in which the tTA-dependent promoter (tetO) drives the expression of ChR2(C128S) (Tanaka et al., 2012). The above two lines were crossed to achieve striatal MSN-specific strong expression of ChR2(C128S). In the compound heterozygous mice strong fluorescent signals spanned the whole projection area of striatal MSNs including the caudate putamen (CPu), the fibers of striatal MSNs and their projection areas including the external segment of the globus pallidus (GP), the entopeduncular nucleus (EP) and the substantia nigra pars reticulata (SNR) (**Figure 2.1A**).

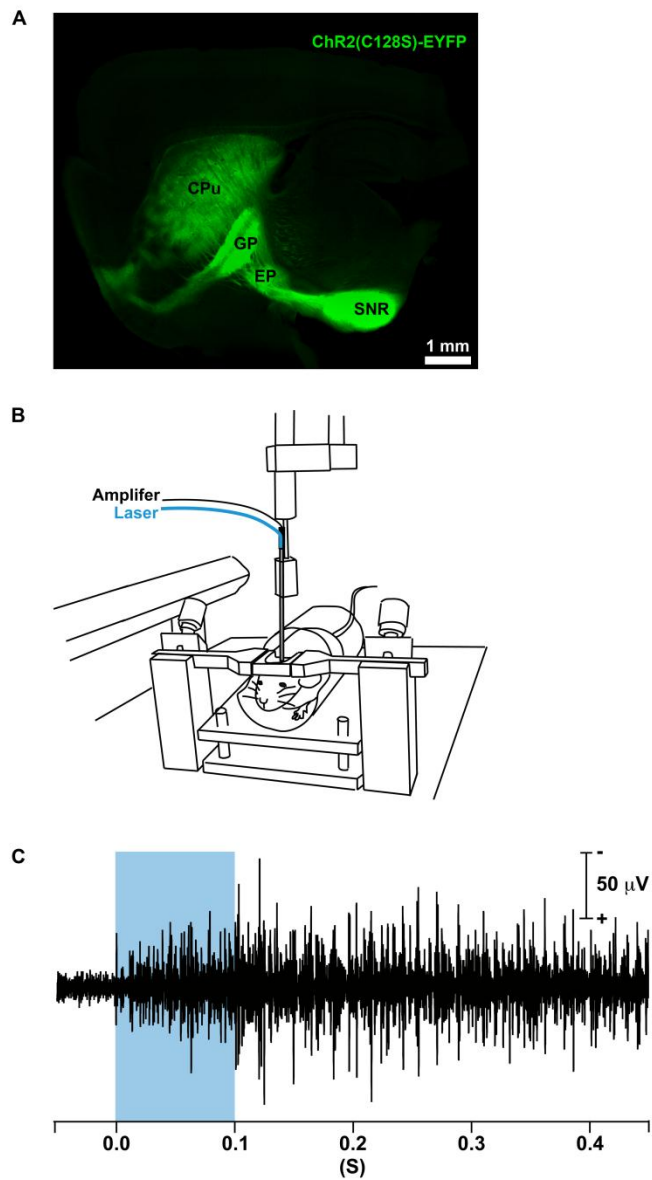


**Figure 2.1. In vivo optical and physiological system for control of striatal MSNs in mice.**

(A) A sagittal section of the mouse brain showing selective expression of ChR2(C128S) in striatal MSNs as visualized by enhanced yellow fluorescent protein

(EYFP) signals. Strong fluorescence was observed in the caudate putamen (CPu) as well as the targets of striatal MSNs such as the external segment of the globus pallidus (GP), the entopeduncular nucleus (EP) and the substantia nigra pars reticulata (SNR).

(B) Schematic of the electrophysiological set-up used for in vivo photostimulation and electrophysiological recordings in awake mice.

(C) A representative electrophysiological recording from the striatum. Photostimulation (a single 100-ms pulse, represented by a blue rectangle) in the striatum evoked neuronal excitation. The excitation lasted more than 1 minute (data not shown). Scale bar: (A) 1 mm.

.....

We recorded extracellular neuronal activity of striatal neurons before and after illuminating with a single 100-ms pulse of blue laser (473 nm) in awake mice (**Figure 2.1B, C**). The laser illumination evoked prolonged excitation which lasted after termination of the photostimulation (**Figure 2.1C**). In our experiment, we used only blue light to modulate neuronal activity. Therefore, the excitation after a single pulse of photostimulation lasted more than 1 minute (data not shown).

To perform in vivo optogenetic manipulation in freely moving animals we implanted optical fibers in the mouse brain targeting the striatum (**Figure 2.2A**). After recovery from implantation procedure mice were kept in their home cages where they did not show any altered behaviors. When awake mice in home cages were given blue light

(a single 500-ms pulse) to illuminate the striatum in one hemisphere, animals displayed complex behaviors, including ipsilateral rotations (Sano and Tanaka, manuscript in preparation). These results indicated that light illumination reliably activated the striatal MSNs and the optogenetic modulation of neuronal excitability was sufficient to trigger recognizable behavioral responses in freely moving mice.

### **Tracing photoactivated neurons**

We looked for a selective increase in expression of IEGs in the ipsilateral striatum after 10 minutes of ChR2(C128S)-mediated unilateral photoactivation in the PDE10A2-tTA mice (**Figure 2.2A**). Any apparent induction of *c-fos*, the most widely used activity marker, was not observed in the striatum in our experimental conditions (**Figure 2.2B1, B1', C**). Therefore, it was necessary to check whether the striatum in the ChR2(C128S)-expressing mice can respond normally to known inducers of IEGs. We found that acute administration of methamphetamine (2 mg/kg, intraperitoneal injection, single dose), which is known to induce IEG expression in the striatum (Wang and McGinty, 1996; Cadet et al., 2001, 2010; Beauvais et al., 2010), significantly upregulated *c-fos* expression in the striatum of the ChR2(C128S)-expressing transgenic mice and the expression pattern was apparently similar to that of wild type mice (**Figure 2.3**). Additionally, our preliminary observation did not indicate any noticeable behavioral difference between the wild type and the transgenic mice without or with methamphetamine treatment (data not

shown). Together, it seemed that the striatal functions were intact in the ChR2(C128S)-expressing PDE10A2-tTA line.

Subsequently, we expanded the screening using a number of IEGs which were found to be induced by brain activities in previous studies. We found strong signals of *Arc* mRNAs in the illuminated striatum (**Figure 2.2B3'**) in addition to very dense signals in other brain regions including the cerebral cortex. Nonetheless, a considerable level of *Arc* mRNA expression was observed also in the contralateral side (**Figure 2.2B3, C**). Similarly, *Junb* expression was only slightly higher in the ipsilateral striatum compared to the contralateral striatum (Data not shown). We found that *Egr1* expression was not suitable for tracing photoactivation of striatal MSNs since dense mRNA signals appeared in both the control and the illuminated hemispheres (**Figure 2.2B4, B4', C**). In addition, any selective induction was absent for other IEGs such as *Fosb*, *Egr3* and *Jun* (Data not shown). In stark contrast, another neuronal IEG, the basic helix-loop-helix (bHLH)-PAS transcription factor *Npas4*, was robustly induced specifically in the ipsilateral striatum following photoactivation of striatal MSNs (**Figure 2.2B2', C**). Signals for *Npas4* mRNAs were almost absent in the contralateral sham-treated striatum (**Figure 2.2B2, C**) and in the striatum of the mice in which optical fibers were implanted in both hemispheres but no laser illumination was done (**Figure 2.4**).

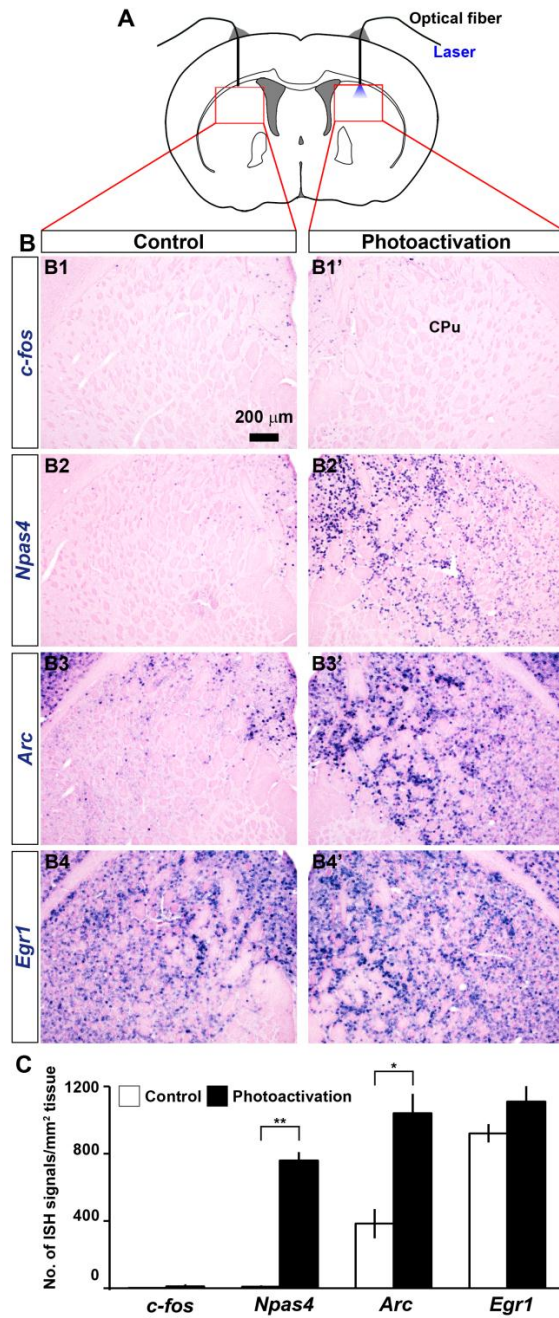


**Figure 2.2. Identification of photoactivated neurons by IEG tracing.**

(A) Schematic used for in vivo photostimulation and histology in the mouse striatum.

Blue light stimulation was given to the left striatum and the right striatum was used

as the sham-treated control. Boxed areas indicate approximate striatal regions shown in B.

(B) Representative images of coronal tissue sections from mice which received optogenetic stimulation in the left striatum showing ISH signals of *c-fos* (B1, B1'), *Npas4* (B2, B2'), *Arc* (B3, B3') and *Egr1* (B4, B4'). CPu, Caudate putamen.

(C) Quantification of *c-fos*, *Npas4*, *Arc* and *Egr1* mRNA signals in the striatum after light stimulation. Induction of *c-fos* was not observed, whereas, a robust increase in *Npas4* mRNA signals appeared in the left striatum which received optogenetic stimulation. Although *Arc* was induced by photostimulation, the expression level was relatively high in the contralateral striatum. Any induction of *Egr1* was not apparent after illumination. Data represent mean  $\pm$  SEM. \*\* Difference between groups was highly significant ( $p \leq 0.01$ ), \* Difference between groups was significant ( $p \leq 0.05$ ).  
Scale bar: (B) 200  $\mu$ m.

.....

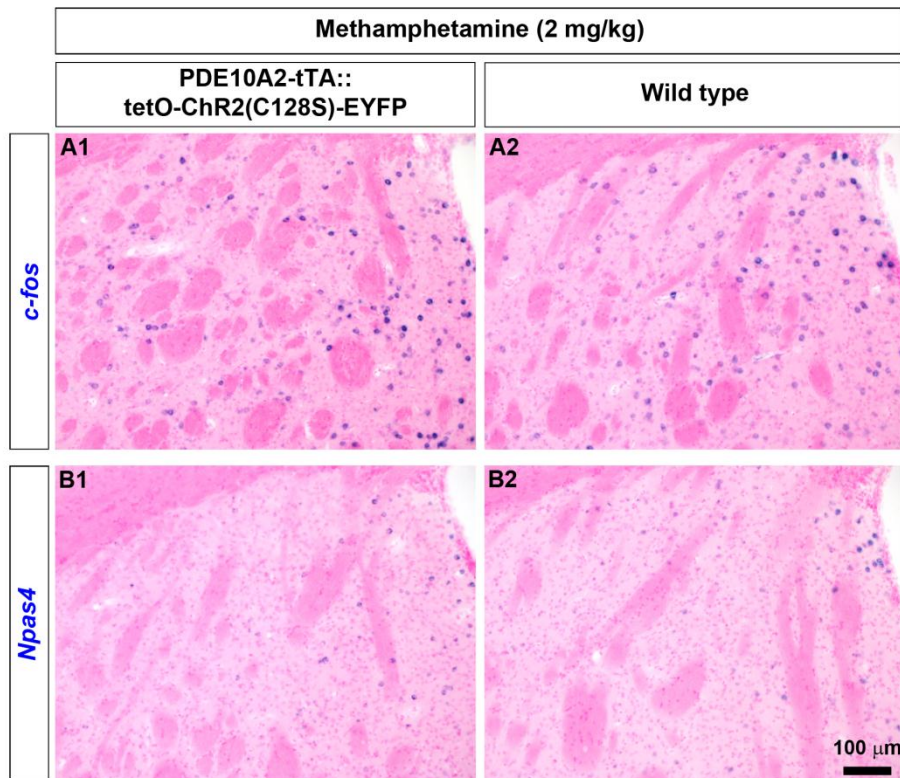


**Figure 2.3. Methamphetamine induced IEG expression in the striatum of the mice which expressed ChR2(C128S) in MSNs.**

(A1, A2) A single dose of methamphetamine (2 mg/kg, i.p.) significantly induced expression of *c-fos* mRNAs in the striatum in both the BAC transgenic (A1) and the wild type mice (A2).

(B1, B2) In both the transgenic (B1) and the wild type mice (B2), *Npas4* was slightly induced after the acute methamphetamine treatment. Scale bar: 100  $\mu\text{m}$ .

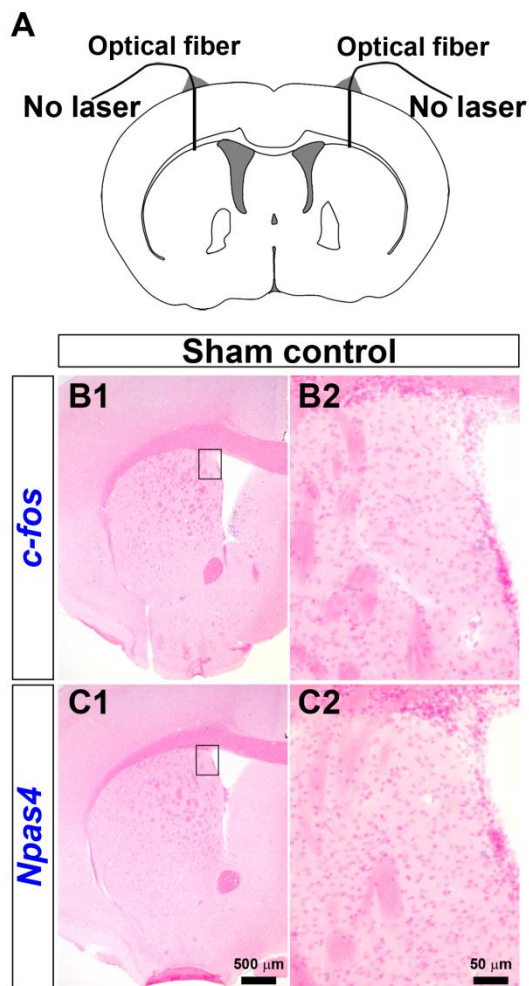


**Figure 2.4. *Npas4* expression was almost absent in the double-instrumented, non-illuminated mice which expressed ChR2(C128S).**

(A) Schematic diagram showing sham control experiments where optical fibers were implanted in both hemispheres but no illumination was given.

(B1-C2) Sham operations did not induce expression of either *c-fos* (B1, B2) or *Npas4* (C1, C2) in the striatum of ChR2(C128S)-expressing mice. Scale bars: (B1, C1) 500 μm, (B2, C2) 50 μm.

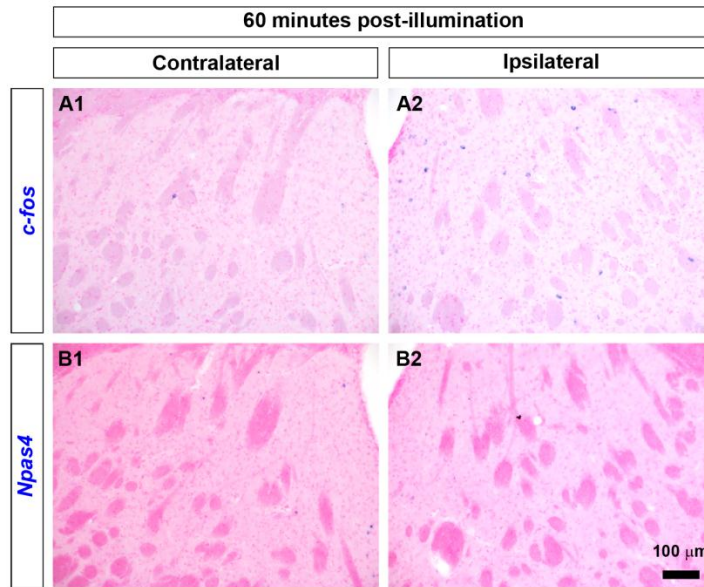


**Figure 2.5. Expression of *c-fos* and *Npas4* in the striatum after 60 minutes of illumination.**

(A1-B2) No significant expression of either *c-fos* (A1, A2) or *Npas4* (B1, B2) was observed in the striatum after 60 minutes of ChR2(C128S)-mediated activation of MSNs. Scale bar: 100  $\mu\text{m}$ .

We also checked IEG induction with an extended time window. In contrast to 10 minutes post-illumination delay, there was almost no ISH signal of *Npas4* mRNA in the striatum after 60 minutes of photoactivation (**Figure 2.5**). These data were consistent with previous studies in respect to the quick and transient induction of *Npas4* (Lin et al., 2008; Ramamoorthi et al., 2011).

In some cases we observed induction of both *Npas4* (see later) and *c-fos* (data not shown) in the ipsilateral cerebral cortex after unilateral optical illumination of the striatum. Such cortical IEG induction was absent in the double-instrumented sham-treated mice (**Figure 2.4B1-C2**). It is possible that the cortical IEG induction we found was secondary effects of striatal stimulation. Previous studies also reported significant induction of *c-fos* expression in the cerebral cortex after striatal stimulation and disinhibition of the thalamocortical pathways has been suggested as a possible mechanism (LaHoste et al., 1996; Sullivan et al., 1996; Mena-Segovia and Giordano, 2003; Gross and Marshall, 2009).

When propagating through a diffuse scattering media like brain tissue the incident light is attenuated resulting from a number of phenomena such as scattering, absorption and conical spreading (Aravanis et al., 2007). Nonetheless, if the target volume is small ( $< 1 \text{ mm}^3$ ) light penetration is not a limiting factor and the entire target could be recruited (Aravanis et al., 2007; Gradinaru et al., 2009). On the other hand, the mouse striatum is a relatively large structure comprising approximately 5-6% of the brain volume (Rosen and Williams, 2001) and it extends approximately 4 mm and 3 mm along the rostrocaudal and dorsoventral axes, respectively (Franklin

and Paxinos, 2007). Presumably, in vivo optogenetic modulation in mouse striatum will recruit a significant volume of tissue proximal to the tip of the optic fiber and may leave the distant regions mostly unaffected. In our experimental conditions light stimulation was applied to the dorsal striatum (**Figure 2.2A**) which has been implicated in motor control (Pisa, 1988; Ebrahimi et al., 1992).

**Figure 2.6** shows expression of *Npas4* as observed in coronal sections of the brain hemisphere ipsilateral to optical illumination. *Npas4* induction took place along the entire mediolateral extent of the striatum near the tip of the optic fiber (**Figure 2.6F**). At the rostral striatum strong induction of *Npas4* appeared mostly in the dorsomedial part (**Figure 2.6B-D**) and expression level was low along the ventral striatum (**Figure 2.6A, B**). It is noteworthy that placement of the optical fiber (both location and orientation/angle of the tip) could influence the number of labeled neurons since the neurons which are distant from the probe may not be activated because of attenuation and conical spreading of the incident light (Aravanis et al., 2007). Nevertheless, we observed reliable photostimulation in our experimental set up and it appeared that optical illumination recruited a substantial volume of striatum along the rostrocaudal, mediolateral and dorsoventral axes as revealed by the selective induction of *Npas4* mRNA expression (**Figure 2.6, Figure 2.7A1-A4**).

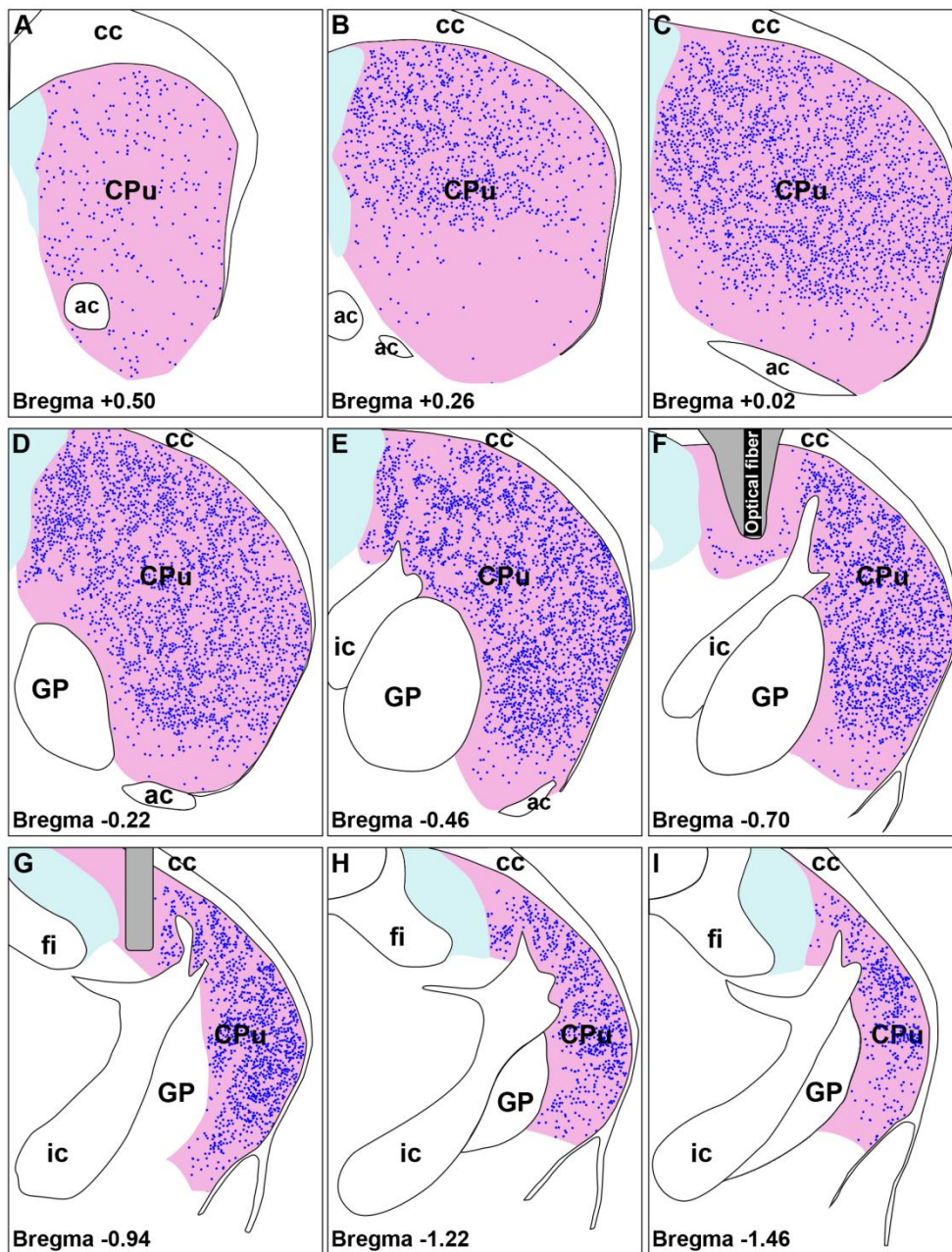


**Figure 2.6. Distribution of *Npas4* ISH signals in the striatum after unilateral blue light illumination.**

Schematic diagrams of the striatum were constructed by superimposing images of stained coronal tissue sections on figures from a standard mouse brain atlas (Franklin

and Paxinos, 2007). *Npas4* ISH signals in the illuminated striatum (CPu) are represented by blue dots. Signals outside the striatum are not shown.

(A-I) Photoactivation-induced expression of *Npas4* in the mouse striatum is shown from bregma + 0.50 mm to bregma – 1.46 mm. The location of the optical fiber is depicted in F. The areas adjacent to the optical fiber appear in gray shade (F, G). (D-H) Strong *Npas4* induction took place in almost the entire extent of the striatal region close to the optical fiber. (A-B) *Npas4* expression level was relatively weaker along the ventral part of the rostral striatum.

ac, Anterior commissure; cc, Corpus callosum; CPu, Caudate putamen; fi, Fimbria of the hippocampus; GP, Globus pallidus; ic, Internal capsule.

.....

Major components of the basal ganglia neuronal network are MSNs, the most abundant cell type in the striatum, and there are several types of interneurons such as cholinergic interneurons and GABAergic interneurons (Kawaguchi et al., 1995; Tepper and Bolam, 2004; Matamales et al., 2009). We performed double fluorescent ISH to know which cell types in the striatum expressed *Npas4* after optical stimulation. In the illuminated striatum almost all *Npas4*-positive cells were double-positive for *Npas4* and *ChR2(C128S)-EYFP* (**Figure 2.7A1-B3**).

Cholinergic interneurons, also known as tonically active neurons (TANs), exhibit spontaneous firing and are synaptically connected with MSNs (Bolam et al., 1984; Chuhma et al., 2011). We used choline acetyltransferase (*Chat*) as a marker for

cholinergic interneurons. It seemed that in cholinergic interneurons induction of *Npas4* was minimal, if any, since none of the *Chat* positive cells (56 cells examined using confocal microscopy) was co-labeled with *Npas4* in the striatum (**Figure 2.7C1-C3**). Seemingly, *Npas4* induction was also absent in parvalbumin (*Pvalb*, also known as PV)-positive GABAergic interneurons as we did not observe any *Pvalb* and *Npas4* double-positive cells (14 cells examined) in the illuminated striatum (**Figure 2.7D1-D3**). Therefore, these data indicated that *Npas4* mRNA expression was induced by photostimulation mostly in the striatal MSNs which expressed ChR2(C128S)-EYFP (**Figure 2.7**).

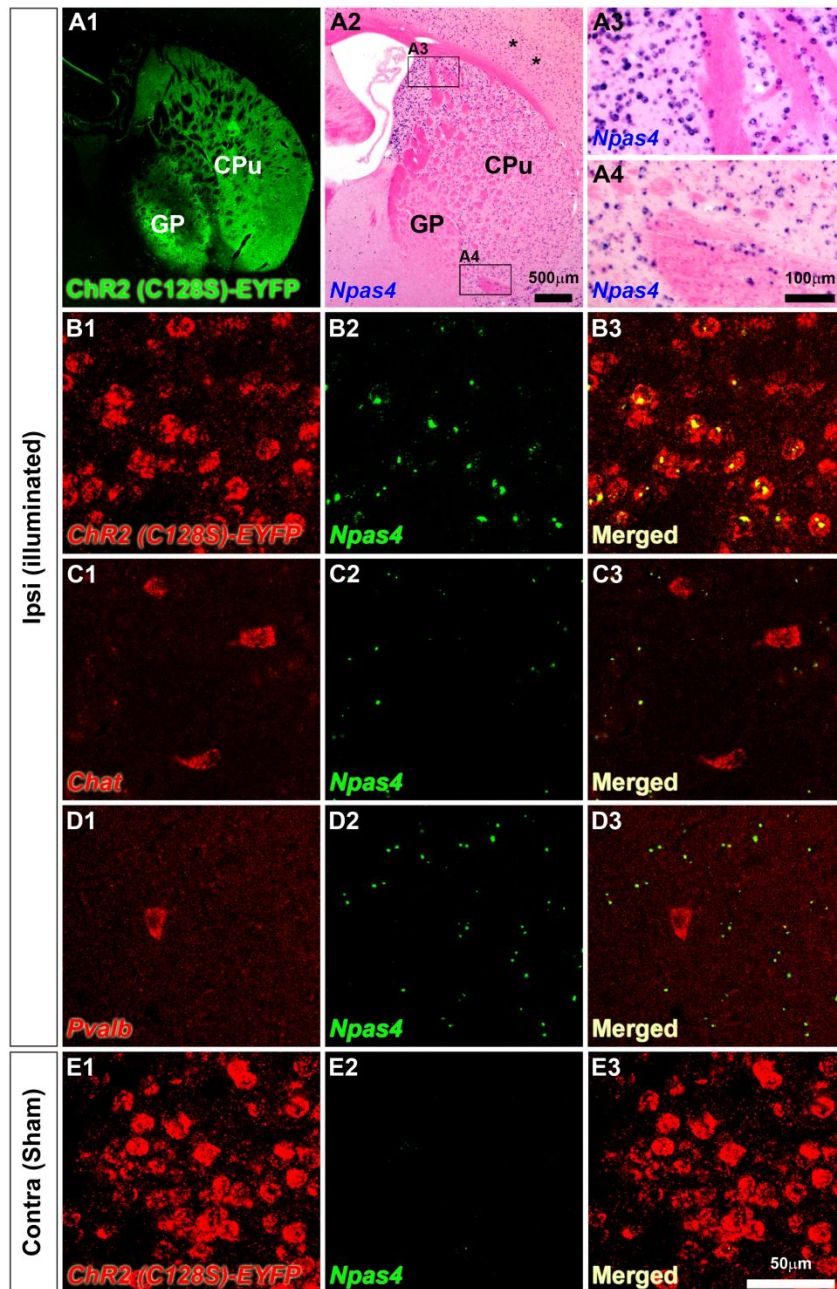


**Figure 2.7. Optical stimulation-induced *Npas4* expression was mostly limited to the ChR2(C128S) expressing MSNs.**

(A1) Fluorescence imaging of coronal tissue section indicates strong expression of the transgene (*ChR2(C128S)-EYFP*) in the striatum. (A2) After unilateral light

stimulation *Npas4* mRNA expression was induced in the ipsilateral striatum (CPu, Caudate putamen). Note that *Npas4* induction was also observed in the cerebral cortex in some cases (asterisks, A2). Boxed areas in A2 are shown in higher magnification in A3 and A4. Induction of *Npas4* was observed from the dorsal (A3) to the ventral (A4) striatum.

(B1-B3) Most of the striatal MSNs expressed the transgene *Chr2(C128S)-EYFP* (B1, red). After illumination *Npas4* (green) was expressed in the ipsilateral striatum (B2). Almost all *Npas4*-expressing cells were co-labeled with *Chr2(C128S)-EYFP* (B3).

(C1-C3) Cholinergic interneurons were identified by *Chat* expression (C1, red). There was almost no co-labeling for *Npas4* (green) and *Chat* (red) (C2, C3).

(D1-D3) *Npas4* (green) mRNA expression was not induced in *Pvalb* (red)-positive GABAergic interneurons.

(E1-E3) Strong expression of *Chr2(C128S)-EYFP* (red) was observed in the contralateral sham-treated striatum (E1, E3) where *Npas4* (green) expression was almost absent (E2, E3).

CPu, Caudate putamen; GP, Globus pallidus. Scale bars: (A1, A2) 500  $\mu\text{m}$ , (A3, A4) 100  $\mu\text{m}$ , (B1-E3) 50  $\mu\text{m}$ .

.....

## Discussion-II

Despite the fact that striatal medium spiny neurons (MSNs) have been strongly implicated in motor control, motivation and habit formation as well as neurological disorders like PD, Huntington's disease (HD), schizophrenia and addiction (Albin et al., 1989; Kreitzer and Malenka, 2008; Bateup et al., 2010), a comprehensive understanding of their biological functions remains a major challenge. In addition to the classical anatomical studies (Smith and Bolam, 1990; Nakano et al., 2000), recent technical advances in neuroscience have started unveiling the intricate connections and functional significance of MSNs (Taverna et al., 2008; Kravitz et al., 2010; Chuhma et al., 2011). Nonetheless, a major obstacle in studying the functions of striatum is the presence of heterogeneous population of MSNs which are intermingled in the basal ganglia networks (Surmeier et al., 2007).

Although intervening striatal activity through optogenetic manipulation can be advantageous in above regards, a precise identification of activated neurons would be necessary to interpret the cellular and behavioral changes which are ensued. In mice, induction of *c-fos* mRNA or Fos immunoreactivity has been used as a proxy for photoactivation of neurons in different brain regions such as the hypothalamus (Lin et al., 2011), the cerebral cortex (Covington et al., 2010) and the striatum (Kravitz et al., 2010). Unexpectedly, we did not observe *c-fos* induction after in vivo unilateral stimulation of the dorsal striatum (**Figure 2.2**). The channelrhodopsin variant ChR2 was used in those previous studies and multiple light pulses were delivered over several minutes whereas we used the channelrhodopsin variant ChR2(C128S) and

applied a single 500-ms pulse of blue light. ChR2 is photodepolarized rapidly and has a moderate channel closing rate while ChR2(C128S) has an increased light sensitivity with a slow off-kinetics (Berndt et al., 2008; Lin, 2010; Schultheis et al., 2011). Consequently, we were convinced that a number of experimental parameters such as the channelrhodopsin variant, number of light pulses and duration of stimulation could account for the absence of *c-fos* mRNA induction in our study. We also found that most of the commonly used IEGs were unsuitable to trace photoactivation in the mouse striatum. We then analyzed expression of *Npas4* which was previously shown to be induced by in vivo sensory stimulation in the visual cortex (Ramamoorthi et al., 2011) and has been implicated in learning and memory (Yun et al., 2010; Ploski et al., 2011). It has been reported that *Npas4* is expressed in different brain regions, selectively in neurons and predominantly in excitatory neurons (Lin et al., 2008). We found that in the striatum *Npas4* expression was very low or absent at the basal condition (**Figure 2.2B2**, **Figure 2.4**). Interestingly, in vivo optical illumination in freely moving mice differentially induced *Npas4* expression specifically in the ipsilateral striatum (**Figure 2.2B2'**).

Can we also expect *Npas4* induction following ChR2(C128S)-mediated photostimulation in other neuronal cell types or other brain regions? Illumination to ChR2(C128S)-expressing hippocampal CA1 neurons resulted in induction of *Npas4* [KFT unpublished data] in addition to *c-fos* induction (Tanaka et al., 2012). However, any induction of *Npas4* was not apparent in raphe neurons where ChR2(C128S) was expressed by taking advantage of the tryptophan hydroxylase 2

(Tph2)-tTA line [KFT, unpublished data]. Thus, induction of a particular IEG, such as *Npas4* and *c-fos*, following optical activation should be assessed for the neuronal cell type of interest.

Differential IEG induction following a given stimulus has also been demonstrated in previous studies (Nguyen et al., 1992; Isogai et al., 2011; Ramamoorthi et al., 2011). Although expression of *Npas4* was found to be selectively induced by membrane depolarization and  $\text{Ca}^{2+}$  influx, *Npas4* was not induced by several neurotrophic factors like BDNF and NT3 which readily induce other transcription factors such as *c-fos* and *Arc* (Lin et al., 2008; Ramamoorthi et al., 2011). It was found that after contextual fear conditioning (CFC) *Npas4* induction took place as early as 5 minutes after training, much earlier than *c-fos* induction and the authors suggested that the pathways which induce *Npas4* expression could be different from those for other IEGs (Ramamoorthi et al., 2011). Therefore, it is possible that in our study optical activation of ChR2(C128S)-expressing striatal MSNs triggered cellular pathways which were sufficient for induction of *Npas4* but not for other IEGs like *c-fos*. Taken together, our results suggest that *Npas4* can be a suitable tracer for identification of photoactivated MSNs at the cellular level in the mouse striatum considering the very low basal expression and a rapid and robust induction following stimulation.

## Conclusion

In this study we first established a set of ISH probes of ten activity-dependent genes, such as *c-fos*, *Arc* and *Egr1*, for detection of neuronal activity in the mouse brain. We show a rapid and transient induction of these genes in the OB following odorant exposure. Notably, our results show for the first time that in vivo olfactory stimulation can strongly induce the neuronal IEG *Npas4* in the mouse OB. We next analyzed CNGA2-deficient male mice in which the olfactory cAMP signaling pathway is almost completely perturbed and the mutants are generally anosmic and sexually unresponsive. An Individual difference in mouse sexual arousal was predictable from IEG induction in the olfactory system of the mutants. Interestingly, *c-fos* was induced robustly in the mutant OB in response to a predator odor although the mice did not show usual avoidance behaviors, suggesting involvement of CNGA2-independent signaling pathway(s) for processing olfactory information.

We next assessed induction of activity-dependent genes in the mouse brain following unilateral optogenetic stimulation of the striatum. Photoactivation was driven by a light-regulated channel protein ChR2(C128S) which was expressed specifically in the striatal MSNs in a transgenic mouse line. Interestingly, commonly used activity markers were unsuitable for identification of photoactivated MSNs due to either no induction or high basal expression, whereas, *Npas4* showed robust and specific induction in the illuminated striatum. Taken together, the ISH probe set we established can be used as a convenient tool for identification of activated neurons at a cellular level in the mouse brain.

## References

- Albin, R.L., Young, A.B., and Penney, J.B. (1989). The functional anatomy of basal ganglia disorders. *Trends in Neurosciences* *12*, 366–375.
- Aravanis, A.M., Wang, L.-P., Zhang, F., Meltzer, L.A., Mogri, M.Z., Schneider, M.B., and Deisseroth, K. (2007). An optical neural interface: in vivo control of rodent motor cortex with integrated fiberoptic and optogenetic technology. *Journal of Neural Engineering* *4*, S143–S156.
- Baker, H., Cummings, D.M., Munger, S.D., Margolis, J.W., Franzen, L., Reed, R.R., and Margolis, F.L. (1999). Targeted deletion of a cyclic nucleotide-gated channel subunit (OCNC1): biochemical and morphological consequences in adult mice. *The Journal of Neuroscience* *19*, 9313–9321.
- Bateup, H.S., Santini, E., Shen, W., Birnbaum, S., Valjent, E., Surmeier, D.J., Fisone, G., Nestler, E.J., and Greengard, P. (2010). Distinct subclasses of medium spiny neurons differentially regulate striatal motor behaviors. *Proceedings of the National Academy of Sciences* *107*, 14845–14850.
- Beauvais, G., Jayanthi, S., McCoy, M.T., Ladenheim, B., and Cadet, J.L. (2010). Differential effects of methamphetamine and SCH23390 on the expression of members of IEG families of transcription factors in the rat striatum. *Brain Research* *1318*, 1–10.
- Belluscio, L., Gold, G.H., Nemes, A., and Axel, R. (1998). Mice Deficient in Golf Are Anosmic. *Neuron* *20*, 69–81.
- Ben-Shaul, Y., Katz, L.C., Mooney, R., and Dulac, C. (2010). In vivo vomeronasal stimulation reveals sensory encoding of conspecific and allospecific cues by the mouse accessory olfactory bulb. *PNAS* *107*, 5172–5177.
- Berndt, A., Yizhar, O., Gunaydin, L.A., Hegemann, P., and Deisseroth, K. (2008). Bi-stable neural state switches. *Nature Neuroscience* *12*, 229–234.
- Bolam, J.P., Wainer, B.H., and Smith, A.D. (1984). Characterization of cholinergic neurons in the rat neostriatum. A combination of choline acetyltransferase immunocytochemistry, Golgi-impregnation and electron microscopy. *Neuroscience* *12*, 711–718.
- Brand, G. (2006). Olfactory/trigeminal interactions in nasal chemoreception. *Neuroscience & Biobehavioral Reviews* *30*, 908–917.

- Brown, M.T.C., Bellone, C., Mameli, M., Labouèbe, G., Bocklisch, C., Balland, B., Dahan, L., Luján, R., Deisseroth, K., and Lüscher, C. (2010). Drug-Driven AMPA Receptor Redistribution Mimicked by Selective Dopamine Neuron Stimulation. *PLoS ONE* 5, e15870.
- Brunet, L.J., Gold, G.H., and Ngai, J. (1996). General Anosmia Caused by a Targeted Disruption of the Mouse Olfactory Cyclic Nucleotide-Gated Cation Channel. *Neuron* 17, 681–693.
- Cadet, J.L., Brannock, C., Krasnova, I.N., Ladenheim, B., McCoy, M.T., Chou, J., Lehrmann, E., Wood, W.H., Becker, K.G., and Wang, Y. (2010). Methamphetamine-Induced Dopamine-Independent Alterations in Striatal Gene Expression in the 6-Hydroxydopamine Hemiparkinsonian Rats. *PLoS ONE* 5, e15643.
- Cadet, J.L., Jayanthi, S., McCoy, M.T., Vawter, M., and Ladenheim, B. (2001). Temporal profiling of methamphetamine-induced changes in gene expression in the mouse brain: evidence from cDNA array. *Synapse* 41, 40–48.
- Capone, F., Venerosi, A., Puopolo, M., Alleva, E., and Cirulli, F. (2005). Behavioral responses of 129/Sv, C57BL/6J and DBA/2J mice to a non-predator aversive olfactory stimulus. *Acta Neurobiol Exp (Wars)* 65, 29–38.
- Castro, F. de (2009). Wiring olfaction: the cellular and molecular mechanisms that guide the development of synaptic connections from the nose to the cortex. *Front. Neurosci.* 3, 52.
- Chiken, S., Shashidharan, P., and Nambu, A. (2008). Cortically Evoked Long-Lasting Inhibition of Pallidal Neurons in a Transgenic Mouse Model of Dystonia. *J. Neurosci.* 28, 13967–13977.
- Chuhma, N., Tanaka, K.F., Hen, R., and Rayport, S. (2011). Functional Connectome of the Striatal Medium Spiny Neuron. *Journal of Neuroscience* 31, 1183–1192.
- Cochran, B.H., Reffel, A.C., and Stiles, C.D. (1983). Molecular cloning of gene sequences regulated by platelet-derived growth factor. *Cell* 33, 939–947.
- Covington, H.E., Lobo, M.K., Maze, I., Vialou, V., Hyman, J.M., Zaman, S., LaPlant, Q., Mouzon, E., Ghose, S., Tamminga, C.A., et al. (2010). Antidepressant Effect of Optogenetic Stimulation of the Medial Prefrontal Cortex. *Journal of Neuroscience* 30, 16082–16090.
- Dhallan, R.S., Yau, K.-W., Schrader, K.A., and Reed, R.R. (1990). Primary structure and functional expression of a cyclic nucleotide-activated channel from olfactory neurons. , Published Online: 13 September 1990; | Doi:10.1038/347184a0 *347*, 184–187.

- Dhungel, S., Masaoka, M., Rai, D., Kondo, Y., and Sakuma, Y. (2011). Both olfactory epithelial and vomeronasal inputs are essential for activation of the medial amygdala and preoptic neurons of male rats. *Neuroscience* *199*, 225–234.
- Ebrahimi, A., Pochet, R., and Roger, M. (1992). Topographical organization of the projections from physiologically identified areas of the motor cortex to the striatum in the rat. *Neuroscience Research* *14*, 39–60.
- Flavell, S.W., and Greenberg, M.E. (2008). Signaling Mechanisms Linking Neuronal Activity to Gene Expression and Plasticity of the Nervous System. *Annual Review of Neuroscience* *31*, 563–590.
- Franklin, K.B.J., and Paxinos, G. (2007). *The Mouse Brain in Stereotaxic Coordinates* (Academic Press).
- Gómez, C., Briñón, J.G., Barbado, M.V., Weruaga, E., Valero, J., and Alonso, J.R. (2005). Heterogeneous targeting of centrifugal inputs to the glomerular layer of the main olfactory bulb. *Journal of Chemical Neuroanatomy* *29*, 238–254.
- Gradinaru, V., Mogri, M., Thompson, K.R., Henderson, J.M., and Deisseroth, K. (2009). Optical deconstruction of parkinsonian neural circuitry. *Science* *324*, 354–359.
- Graybiel, A.M., Moratalla, R., and Robertson, H.A. (1990). Amphetamine and cocaine induce drug-specific activation of the c-fos gene in striosome-matrix compartments and limbic subdivisions of the striatum. *Proceedings of the National Academy of Sciences* *87*, 6912–6916.
- Greenberg, M.E., and Ziff, E.B. (1984). Stimulation of 3T3 cells induces transcription of the c-fos proto-oncogene. *Nature* *311*, 433–438.
- Gross, N.B., and Marshall, J.F. (2009). Striatal dopamine and glutamate receptors modulate methamphetamine-induced cortical Fos expression. *Neuroscience* *161*, 1114–1125.
- Guthrie, K.M., Anderson, A.J., Leon, M., and Gall, C. (1993). Odor-induced increases in c-fos mRNA expression reveal an anatomical “unit” for odor processing in olfactory bulb. *Proceedings of the National Academy of Sciences* *90*, 3329–3333.
- Hoffman, G.E., and Lyo, D. (2002). Anatomical Markers of Activity in Neuroendocrine Systems: Are we all “Fos-ed out”? *Journal of Neuroendocrinology* *14*, 259–268.
- Inaki, K., Takahashi, Y.K., Nagayama, S., and Mori, K. (2002). Molecular-feature domains with posterodorsal–anteroventral polarity in the symmetrical sensory maps

of the mouse olfactory bulb: mapping of odourant-induced Zif268 expression. *European Journal of Neuroscience* *15*, 1563–1574.

Isogai, Y., Si, S., Pont-Lezica, L., Tan, T., Kapoor, V., Murthy, V.N., and Dulac, C. (2011). Molecular organization of vomeronasal chemoreception. *Nature* *478*, 241–245.

Johnson, B.A., Farahbod, H., Xu, Z., Saber, S., and Leon, M. (2004). Local and global chemotopic organization: General features of the glomerular representations of aliphatic odorants differing in carbon number. *The Journal of Comparative Neurology* *480*, 234–249.

Kaupp, U.B. (2010). Olfactory signalling in vertebrates and insects: differences and commonalities. *Nature Reviews Neuroscience* *11*, 188–200.

Kawaguchi, Y., Wilson, C.J., Augood, S.J., and Emson, P.C. (1995). Striatal interneurons: chemical, physiological and morphological characterization. *Trends in Neurosciences* *18*, 527–535.

Keller, M., Baum, M.J., Brock, O., Brennan, P.A., and Bakker, J. (2009). The main and the accessory olfactory systems interact in the control of mate recognition and sexual behavior. *Behavioural Brain Research* *200*, 268–276.

Kippin, T., Cain, S., and Pfau, J. (2003). Estrous odors and sexually conditioned neutral odors activate separate neural pathways in the male rat. *Neuroscience* *117*, 971–979.

Kiselycznyk, C.L., Zhang, S., and Linster, C. (2006). Role of centrifugal projections to the olfactory bulb in olfactory processing. *Learning & Memory* *13*, 575–579.

Kobayakawa, K., Kobayakawa, R., Matsumoto, H., Oka, Y., Imai, T., Ikawa, M., Okabe, M., Ikeda, T., Itohara, S., Kikusui, T., et al. (2007). Innate versus learned odour processing in the mouse olfactory bulb. *Nature* *450*, 503–508.

Kovács, K.J. (2008). Measurement of Immediate-Early Gene Activation- c-fos and Beyond. *Journal of Neuroendocrinology* *20*, 665–672.

Kratskin, I., Hummel, T., Hastings, L., and Doty, R. (2000). 3-Methylindole alters both olfactory and trigeminal nasal mucosal potentials in rats. *Neuroreport* *11*, 2195–2197.

Kravitz, A.V., Freeze, B.S., Parker, P.R.L., Kay, K., Thwin, M.T., Deisseroth, K., and Kreitzer, A.C. (2010). Regulation of parkinsonian motor behaviours by optogenetic control of basal ganglia circuitry. *Nature* *466*, 622–626.

- Kreitzer, A.C., and Malenka, R.C. (2008). Striatal Plasticity and Basal Ganglia Circuit Function. *Neuron* 60, 543–554.
- LaHoste, G.J., Ruskin, D.N., and Marshall, J.F. (1996). Cerebrocortical Fos expression following dopaminergic stimulation: D1/D2 synergism and its breakdown. *Brain Research* 728, 97–104.
- Lecoq, J., Tiret, P., and Charpak, S. (2009). Peripheral Adaptation Codes for High Odor Concentration in Glomeruli. *Journal of Neuroscience* 29, 3067–3072.
- Lehr, H.-A., Loss, C.M. van der, Teeling, P., and Gown, A.M. (1999). Complete Chromogen Separation and Analysis in Double Immunohistochemical Stains Using Photoshop-based Image Analysis. *J Histochem Cytochem* 47, 119–125.
- Leinders-Zufall, T., Cockerham, R.E., Michalakis, S., Biel, M., Garbers, D.L., Reed, R.R., Zufall, F., and Munger, S.D. (2007). Contribution of the receptor guanylyl cyclase GC-D to chemosensory function in the olfactory epithelium. *Proceedings of the National Academy of Sciences* 104, 14507–14512.
- Leslie, J.H., and Nedivi, E. (2011). Activity-regulated genes as mediators of neural circuit plasticity. *Progress in Neurobiology* 94, 223–237.
- Lin, D., Boyle, M.P., Dollar, P., Lee, H., Lein, E.S., Perona, P., and Anderson, D.J. (2011). Functional identification of an aggression locus in the mouse hypothalamus. *Nature* 470, 221–226.
- Lin, D.M., and Ngai, J. (1999). Development of the vertebrate main olfactory system. *Current Opinion in Neurobiology* 9, 74–78.
- Lin, J.Y. (2010). A user's guide to channelrhodopsin variants: features, limitations and future developments. *Experimental Physiology* 96, 19–25.
- Lin, W., Arellano, J., Slotnick, B., and Restrepo, D. (2004). Odors Detected by Mice Deficient in Cyclic Nucleotide-Gated Channel Subunit A2 Stimulate the Main Olfactory System. *J. Neurosci.* 24, 3703–3710.
- Lin, W., Margolskee, R., Donnert, G., Hell, S.W., and Restrepo, D. (2007). Olfactory neurons expressing transient receptor potential channel M5 (TRPM5) are involved in sensing semiochemicals. *Proceedings of the National Academy of Sciences* 104, 2471–2476.
- Lin, Y., Bloodgood, B.L., Hauser, J.L., Lapan, A.D., Koon, A.C., Kim, T.-K., Hu, L.S., Malik, A.N., and Greenberg, M.E. (2008). Activity-dependent regulation of inhibitory synapse development by Npas4. *Nature* 455, 1198–1204.

- Lledo, P.-M., Gheusi, G., and Vincent, J.-D. (2005). Information Processing in the Mammalian Olfactory System. *Physiol Rev* 85, 281–317.
- Mandiyani, V.S., Coats, J.K., and Shah, N.M. (2005). Deficits in sexual and aggressive behaviors in *Cnga2* mutant mice. *Nature Neuroscience* 8, 1660–1662.
- Masahira, N., Takebayashi, H., Ono, K., Watanabe, K., Ding, L., Furusho, M., Ogawa, Y., Nabeshima, Y., Alvarez-Buylla, A., Shimizu, K., et al. (2006). Olig2-positive progenitors in the embryonic spinal cord give rise not only to motoneurons and oligodendrocytes, but also to a subset of astrocytes and ependymal cells. *Developmental Biology* 293, 358–369.
- Matamales, M., Bertran-Gonzalez, J., Salomon, L., Degos, B., Deniau, J.-M., Valjent, E., Hervé, D., and Girault, J.-A. (2009). Striatal Medium-Sized Spiny Neurons: Identification by Nuclear Staining and Study of Neuronal Subpopulations in BAC Transgenic Mice. *PLoS ONE* 4, e4770.
- Matsumoto, H., Kobayakawa, K., Kobayakawa, R., Tashiro, T., Mori, K., Sakano, H., and Mori, K. (2010). Spatial Arrangement of Glomerular Molecular-Feature Clusters in the Odorant-Receptor Class Domains of the Mouse Olfactory Bulb. *J Neurophysiol* 103, 3490–3500.
- Matsutani, S., and Yamamoto, N. (2008). Centrifugal innervation of the mammalian olfactory bulb. *Anatomical Science International* 83, 218–227.
- Mena-Segovia, J., and Giordano, M. (2003). Striatal dopaminergic stimulation produces c-Fos expression in the PPT and an increase in wakefulness. *Brain Research* 986, 30–38.
- Mofidi, R., Walsh, R., Ridgway, P., Crotty, T., McDermott, E., Keaveny, T., Duffy, M., Hill, A.D., and O'Higgins, N. (2003). Objective measurement of breast cancer oestrogen receptor status through digital image analysis. *European Journal of Surgical Oncology (EJSO)* 29, 20–24.
- Mombaerts, P. (2006). Axonal Wiring in the Mouse Olfactory System. *Annual Review of Cell and Developmental Biology* 22, 713–737.
- Mombaerts, P., Wang, F., Dulac, C., Chao, S.K., Nemes, A., Mendelsohn, M., Edmondson, J., and Axel, R. (1996). Visualizing an Olfactory Sensory Map. *Cell* 87, 675–686.
- Mori, K., and Sakano, H. (2011). How Is the Olfactory Map Formed and Interpreted in the Mammalian Brain? *Annual Review of Neuroscience* 34, 467–499.

- Mori, K., Takahashi, Y.K., Igarashi, K.M., and Yamaguchi, M. (2006). Maps of Odorant Molecular Features in the Mammalian Olfactory Bulb. *Physiol Rev* 86, 409–433.
- Nakano, K., Kayahara, T., Tsutsumi, T., and Ushiro, H. (2000). Neural circuits and functional organization of the striatum. *Journal of Neurology* 247, 1–15.
- Nestler, E.J. (2001). Molecular basis of long-term plasticity underlying addiction. *Nat. Rev. Neurosci.* 2, 119–128.
- Nguyen, T.V., Kosofsky, B.E., Birnbaum, R., Cohen, B.M., and Hyman, S.E. (1992). Differential expression of c-fos and zif268 in rat striatum after haloperidol, clozapine, and amphetamine. *Proceedings of the National Academy of Sciences* 89, 4270–4274.
- Okuno, H. (2011). Regulation and function of immediate-early genes in the brain: Beyond neuronal activity markers. *Neuroscience Research* 69, 175–186.
- Pírez, N., and Wachowiak, M. (2008). In Vivo Modulation of Sensory Input to the Olfactory Bulb by Tonic and Activity-Dependent Presynaptic Inhibition of Receptor Neurons. *J. Neurosci.* 28, 6360–6371.
- Pisa, M. (1988). Motor somatotopy in the striatum of rat: Manipulation, biting and gait. *Behavioural Brain Research* 27, 21–35.
- Ploski, J.E., Monsey, M.S., Nguyen, T., DiLeone, R.J., and Schafe, G.E. (2011). The Neuronal PAS Domain Protein 4 (Npas4) Is Required for New and Reactivated Fear Memories. *PLoS ONE* 6, e23760.
- Ramamoorthi, K., Fropf, R., Belfort, G.M., Fitzmaurice, H.L., McKinney, R.M., Neve, R.L., Otto, T., and Lin, Y. (2011). Npas4 Regulates a Transcriptional Program in CA3 Required for Contextual Memory Formation. *Science* 334, 1669–1675.
- Ressler, K.J., Sullivan, S.L., and Buck, L.B. (1993). A zonal organization of odorant receptor gene expression in the olfactory epithelium. *Cell* 73, 597–609.
- Ressler, K.J., Sullivan, S.L., and Buck, L.B. (1994). Information coding in the olfactory system: Evidence for a stereotyped and highly organized epitope map in the olfactory bulb. *Cell* 79, 1245–1255.
- Restrepo, D., Arellano, J., Oliva, A.M., Schaefer, M.L., and Lin, W. (2004). Emerging views on the distinct but related roles of the main and accessory olfactory systems in responsiveness to chemosensory signals in mice. *Hormones and Behavior* 46, 247–256.

- Ronnett, G.V., and Moon, C. (2002). G Proteins and Olfactory Signal Transduction. *Annual Review of Physiology* 64, 189–222.
- Rosen, G., and Williams, R. (2001). Complex trait analysis of the mouse striatum: independent QTLs modulate volume and neuron number. *BMC Neuroscience* 2, 5.
- Rubin, B.D., and Katz, L.C. (1999). Optical Imaging of Odorant Representations in the Mammalian Olfactory Bulb. *Neuron* 23, 499–511.
- Sakano, H. (2010). Neural Map Formation in the Mouse Olfactory System. *Neuron* 67, 530–542.
- Sallaz, M., and Jourdan, F. (1996). Odour-induced c-fos expression in the rat olfactory bulb: involvement of centrifugal afferents. *Brain Research* 721, 66–75.
- Sano, H., and Yokoi, M. (2007). Striatal Medium Spiny Neurons Terminate in a Distinct Region in the Lateral Hypothalamic Area and Do Not Directly Innervate Orexin/Hypocretin- or Melanin-Concentrating Hormone-Containing Neurons. *Journal of Neuroscience* 27, 6948–6955.
- Schaefer, M.L., Böttger, B., Silver, W.L., and Finger, T.E. (2002). Trigeminal collaterals in the nasal epithelium and olfactory bulb: A potential route for direct modulation of olfactory information by trigeminal stimuli. *The Journal of Comparative Neurology* 444, 221–226.
- Schoenenberger, P., Gerosa, D., and Oertner, T.G. (2009). Temporal control of immediate early gene induction by light. *PLoS One* 4, e8185.
- Schultheis, C., Liewald, J.F., Bamberg, E., Nagel, G., and Gottschalk, A. (2011). Optogenetic Long-Term Manipulation of Behavior and Animal Development. *PLoS ONE* 6, e18766.
- Serizawa, S., Miyamichi, K., Takeuchi, H., Yamagishi, Y., Suzuki, M., and Sakano, H. (2006). A Neuronal Identity Code for the Odorant Receptor-Specific and Activity-Dependent Axon Sorting. *Cell* 127, 1057–1069.
- Sheng, M., and Greenberg, M.E. (1990). The regulation and function of c-fos and other immediate early genes in the nervous system. *Neuron* 4, 477–485.
- Smith, A.D., and Bolam, J.P. (1990). The neural network of the basal ganglia as revealed by the study of synaptic connections of identified neurones. *Trends Neurosci.* 13, 259–265.
- Spehr, M., and Munger, S.D. (2009). Olfactory receptors: G protein-coupled receptors and beyond. *Journal of Neurochemistry* 109, 1570–1583.

- Stettler, D.D., and Axel, R. (2009). Representations of Odor in the Piriform Cortex. *Neuron* 63, 854–864.
- Sullivan, A.M., Reynolds, D.S., Thomas, K.L., and Morton, A.J. (1996). Cortical induction of c-fos by intrastriatal endothelin-1 is mediated via NMDA receptors. *Neuroreport* 8, 211–216.
- Surmeier, D.J., Ding, J., Day, M., Wang, Z., and Shen, W. (2007). D1 and D2 dopamine-receptor modulation of striatal glutamatergic signaling in striatal medium spiny neurons. *Trends in Neurosciences* 30, 228–235.
- Takahashi, L.K., Nakashima, B.R., Hong, H., and Watanabe, K. (2005). The smell of danger: A behavioral and neural analysis of predator odor-induced fear. *Neuroscience & Biobehavioral Reviews* 29, 1157–1167.
- Tanaka, K.F., Matsui, K., Sasaki, T., Sano, H., Sugio, S., Fan, K., Hen, R., Nakai, J., Yanagawa, Y., Hasuwa, H., et al. (2012). Expanding the Repertoire of Optogenetically Targeted Cells with an Enhanced Gene Expression System. *Cell Reports* 2, 397–406.
- Taverna, S., Ilijic, E., and Surmeier, D.J. (2008). Recurrent Collateral Connections of Striatal Medium Spiny Neurons Are Disrupted in Models of Parkinson's Disease. *J. Neurosci.* 28, 5504–5512.
- Tepper, J.M., and Bolam, J.P. (2004). Functional diversity and specificity of neostriatal interneurons. *Current Opinion in Neurobiology* 14, 685–692.
- Trinh, K., and Storm, D.R. (2003). Vomeronasal organ detects odorants in absence of signaling through main olfactory epithelium. *Nature Neuroscience* 6, 519–525.
- Uchida, N., Takahashi, Y.K., Tanifuji, M., and Mori, K. (2000). Odor maps in the mammalian olfactory bulb: domain organization and odorant structural features. *Nature Neuroscience* 3, 1035–1043.
- Usui, N., Watanabe, K., Ono, K., Tomita, K., Tamamaki, N., Ikenaka, K., and Takebayashi, H. (2012). Role of motoneuron-derived neurotrophin 3 in survival and axonal projection of sensory neurons during neural circuit formation. *Development* 139, 1125–1132.
- Vassar, R., Ngai, J., and Axel, R. (1993). Spatial segregation of odorant receptor expression in the mammalian olfactory epithelium. *Cell* 74, 309–318.
- Waldeck, C., Vocke, K., Ungerer, N., Frings, S., and Möhrlein, F. (2009). Activation and desensitization of the olfactory cAMP-gated transduction channel: identification of functional modules. *J Gen Physiol* 134, 397–408.

- Wang, F., Nemes, A., Mendelsohn, M., and Axel, R. (1998). Odorant Receptors Govern the Formation of a Precise Topographic Map. *Cell* 93, 47–60.
- Wang, J.Q., and McGinty, J.F. (1996). Acute methamphetamine-induced *zif/268*, *preprodynorphin*, and *preproenkephalin* mRNA expression in rat striatum depends on activation of NMDA and kainate/AMPA receptors. *Brain Res. Bull.* 39, 349–357.
- Wen, L., Wang, H., Tanimoto, S., Egawa, R., Matsuzaka, Y., Mushiake, H., Ishizuka, T., and Yawo, H. (2010). Opto-Current-Clamp Actuation of Cortical Neurons Using a Strategically Designed Channelrhodopsin. *PLoS ONE* 5, e12893.
- Wong, S.T., Trinh, K., Hacker, B., Chan, G.C.K., Lowe, G., Gaggar, A., Xia, Z., Gold, G.H., and Storm, D.R. (2000). Disruption of the Type III Adenylyl Cyclase Gene Leads to Peripheral and Behavioral Anosmia in Transgenic Mice. *Neuron* 27, 487–497.
- Xu, F., Schaefer, M., Kida, I., Schafer, J., Liu, N., Rothman, D.L., Hyder, F., Restrepo, D., and Shepherd, G.M. (2005). Simultaneous activation of mouse main and accessory olfactory bulbs by odors or pheromones. *The Journal of Comparative Neurology* 489, 491–500.
- Yizhar, O., Fenno, L.E., Davidson, T.J., Mogri, M., and Deisseroth, K. (2011). Optogenetics in Neural Systems. *Neuron* 71, 9–34.
- Yun, J., Koike, H., Ibi, D., Toth, E., Mizoguchi, H., Nitta, A., Yoneyama, M., Ogita, K., Yoneda, Y., Nabeshima, T., et al. (2010). Chronic restraint stress impairs neurogenesis and hippocampus-dependent fear memory in mice: possible involvement of a brain-specific transcription factor *Npas4*. *Journal of Neurochemistry* 114, 1840–1851.
- Zhao, H., Ivic, L., Otaki, J.M., Hashimoto, M., Mikoshiba, K., and Firestein, S. (1998). Functional Expression of a Mammalian Odorant Receptor. *Science* 279, 237–242.